Vaccination with tumor-ganglioside glycomimetics activates a selective immunity that affords cancer therapy

Tong, Wenyong; Maira, Mario; Roychoudhury, Rajarshi; Galan, Alba; Brahimi, Fouad; Gilbert, Michel; Cunningham, Anna-Maria; Josephy, Sylvia; Pirvulescu, Iulia; Moffett, Serge; Saragovi, H. Uri

Publisher's version / Version de l'éditeur:
https://doi.org/10.1016/j.chembiol.2019.03.018
Cell Chemical Biology, 26, 7, pp. 1013-1026.e4, 2019-05-16

Article

Cell Chemical Biology

Vaccination with Tumor-Ganglioside Glycomimetics Activates a Selective Immunity that Affords Cancer Therapy

Graphical Abstract

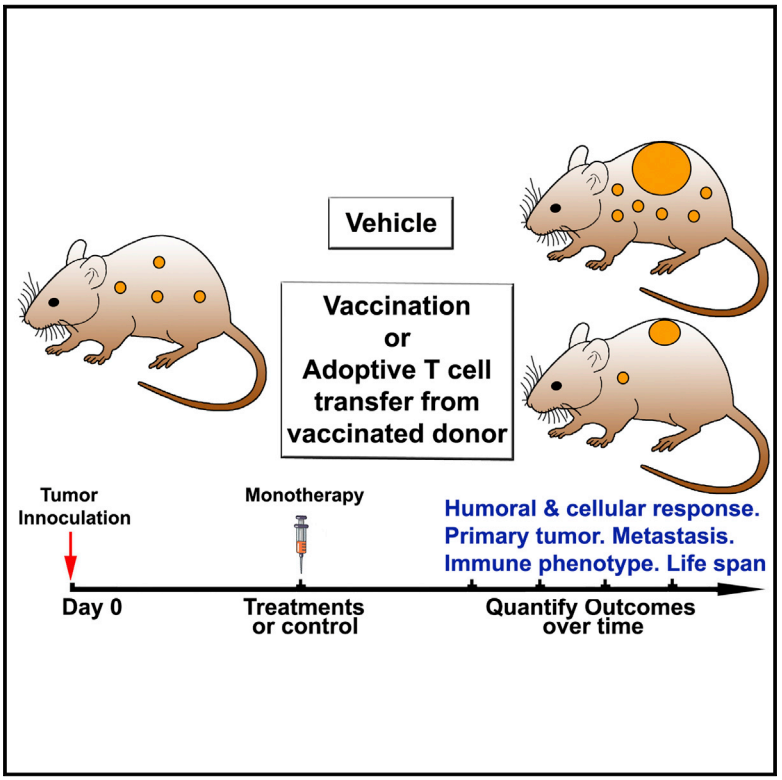

Authors

Wenyong Tong, Mario Maira, Rajarshi Roychoudhury, ..., Iulia Pirvulescu, Serge Moffett, H. Uri Saragovi

Correspondence

uri.saragovi@mcgill.ca

In Brief

Tong et al. show that a carbohydrate mimetic can act as an immunogenic vaccine that activates humoral and cellular immunity.

Highlights

- Class-switching immunoglobulins
- Expanded $CD8^+$ and $\delta\gamma$ T cells that become TILs
- Reduced primary tumor and metastasis
- Effective in a therapeutic modality, injected after tumor

Tong et al., 2019, Cell Chemical Biology *26*, 1013–1026
July 18, 2019
https://doi.org/10.1016/j.chembiol.2019.03.018

CellPress

Cell Chemical Biology
Article

Vaccination with Tumor-Ganglioside Glycomimetics Activates a Selective Immunity that Affords Cancer Therapy

Wenyong Tong,[1,2,4] Mario Maira,[1,4] Rajarshi Roychoudhury,[1,4] Alba Galan,[1] Fouad Brahimi,[1] Michel Gilbert,[3] Anna-Maria Cunningham,[3] Sylvia Josephy,[1] Iulia Pirvulescu,[1,2] Serge Moffett,[1] and H. Uri Saragovi[1,2,5,*]
[1]Lady Davis Institute-Jewish General Hospital, 3755 Côte St. Catherine, E-535, Montreal, QC H3T 1E2, Canada
[2]Pharmacology and Therapeutics, McGill University, Montreal, QC H3G 1Y6, Canada
[3]Human Health Therapeutics Research Centre, National Research Council of Canada, Ottawa K1A 0R6, Canada
[4]These authors contributed equally
[5]Lead Contact
*Correspondence: uri.saragovi@mcgill.ca
https://doi.org/10.1016/j.chembiol.2019.03.018

SUMMARY

Immune targeting of (glyco)protein tumor markers has been useful to develop cancer and virus vaccines. However, the ganglioside family of tumor-associated glycolipids remains intractable to vaccine approaches. Here we show that synthetic antigens mimicking the carbohydrate moiety of GD2 or GD3 gangliosides can be used as vaccines to activate a selective humoral and cellular immunity that is therapeutic against several cancers expressing GD2 or GD3. Adoptive transfer of T cells generated after vaccination elicits tumor-infiltrating lymphocytes of the γδ T cell receptor and CD8$^+$ phenotypes; and affords a high therapeutic index. The glycomimetic vaccine principles can be expanded to target the family of tumor gangliosides and other carbohydrates expressed primarily in pathological states.

INTRODUCTION

Gangliosides are sialic acid-containing glycosphingolipids with an extracellular carbohydrate headgroup linked to a ceramide with two lipid tails embedded in the outer leaflet of the plasma membrane. The unique extracellular carbohydrate head defines the name of each ganglioside (Figure S1), while the lipids are heterogeneous and variable within a ganglioside.

Some gangliosides such as GM1 are ubiquitous and appear in most normal cells, but tumor-marker gangliosides (TMGs) such as GD2 and GD3 are TMGs expressed at high levels in cancer (Daniotti et al., 2013, 2016; Gagnon and Saragovi, 2002) such as neuroblastoma, melanoma, lymphomas, small cell lung cancer, gliomas, breast cancer stem cells, and other pathologies.

Functionally, TMGs provide tumors with advantages in growth, metastasis (Cazet et al., 2009; Shibuya et al., 2012), and enhanced angiogenesis and blood supply, allowing them to extravasate (Liu et al., 2006; Ziche et al., 1992). TMGs can promote tyrosine kinase signal transduction (Tong et al., 2015); interact with adhesion proteins; and regulate raft, cell-cell, and cell-matrix interactions (Aixinjueluo et al., 2005; Furukawa et al., 2006; Gagnon and Saragovi, 2002; Hamamura et al., 2011; Iwabuchi et al., 2000; Nakashima et al., 2007; Todeschini et al., 2007; Tong et al., 2015; Yoshida et al., 2002), making TMGs etiological for cancer. Also, TMGs afford tumors with the ability to evade the immune system. GD2 and GD3 are immunosuppressive (Grayson and Ladisch, 1992) and suppress antigen presentation (Caldwell et al., 2003; Shurin et al., 2001; Yoshida et al., 2001).

Therefore, the TMGs are etiological in cancer development and immune evasion, making them valuable targets. The TMG family, which is a subset of tumor-associated carbohydrate antigens, comprises >20 glycosphingolipids highly expressed in many cancer types for which a therapeutic strategy could be developed (Heimburg-Molinaro et al., 2011). From a translational medicine perspective, the pattern of TMG expression is conserved across mammalian species, the glycan structures that define each TMG are maintained (e.g., the GD2 carbohydrate tree is identical in mouse and humans), TMG expression in tumor cells is homogeneous and uniform in cell lines and primary tumors (Doronin et al., 2014), and expression of TMGs does not downregulate during or after therapy at least in osteosarcoma and glioblastoma (Poon et al., 2015). These features make TMGs attractive not just as tumor markers but also as relevant etiological targets for cancer therapy, and they have thus been prioritized (Cheever et al., 2009).

However, exploiting TMGs using immunotherapy has been challenging because glycolipids are poor immunogens. The carbohydrate may not be efficiently processed or presented in the context of major histocompatibility complex (MHC)/human leukocyte antigen (Heimburg-Molinaro et al., 2011; Sun et al., 2016); and while lipids can be recognized by specialized CD1-restricted T cells (TCRαβ or TCRγδ or natural killer T cells [NK-T]) (Brigl and Brenner, 2004; Park et al., 2008; Van Rhijn et al., 2016), each lipid is not unique to a specific TMG, causing concerns of possible tolerance or cross-reactivity.

Notwithstanding the challenges above, GD2 and GD3 have been exploited clinically as tumor targets. Partial success in cancer therapy was achieved by administering monoclonal antibodies (mAbs) anti-GD2 (Cheung et al., 1998; Saleh et al., 1992;

Yu et al., 2010) or anti-GD3 (Bajorin et al., 1990; Minasian et al., 1995; Vadhan-Raj et al., 1988) in combination with chemotherapy or as a bifunctional antibody (Yankelevich et al., 2012; Yu et al., 2010). Strategies somewhat related to passive immunity comprise mimotopes and anti-idiotypes (Bleeke et al., 2009; Fest et al., 2006; Horwacik et al., 2011; Kozbor, 2010; Wondimu et al., 2008), and engineered chimeric antigen receptors of an anti-GD2 mAb sequence expressed in T cells or NK cells (Esser et al., 2012). Unfortunately, all of these produced poor results and exhibited low therapeutic efficacy and a low therapeutic index due to side effects (Navid et al., 2010); however, dinutuximab (Ch14.18 mAb) was approved for high-risk neuroblastoma, with other trials ongoing for neuroblastoma (NCT01822652, NCT02107963) and advanced sarcomas (NCT01953900).

Active immunization using vaccines also generated poor outcomes. We noted that most vaccines conjugated native gangliosides (containing heterogeneous lipids) to carriers (Chapman et al., 2000; Kawashima et al., 2003; Kim et al., 2011; Ragupathi et al., 2000, 2002, 2003), and the chemical conjugation caused further heterogeneity (Astronomo and Burton, 2010; Danishefsky and Allen, 2000). The most immunogenic vaccine conjugate did not provide clinical benefits (Kirkwood et al., 2001).

We also noted that the ganglioside vaccines were thought to elicit antibodies acting via complement-dependent cytotoxicity. However, the antibody responses to gangliosides may be short-lived (Chapman et al., 2004; Ragupathi et al., 2000), and there was no direct correlation between anti-ganglioside antibody titer and tumor therapy (Bleeke et al., 2009; Hakomori, 2001; Navid et al., 2010; Terme et al., 2014).

We further noted that all ganglioside vaccines reported humoral response (e.g., testing antisera after vaccination) but failed to report on cellular immunity. This astonishing bias may be attributed to the relative success of passive therapy using anti-GD2 and anti-GD3 antibodies; but may have been conceptually misleading.

As an alternative, we proposed to explore the generation of carbohydrate-specific T cells. Our hypothesis was that a multivalent structure mimicking the aggregated state of TMGs within rafts, and sized to fit immune binding pockets, may be crucial for a T cell response. We produced a synthetic vaccine using GD2 or GD3 glycomimetic analogs on a dendrimer core. The glycomimetic precursors (Blixt et al., 2005; Tong et al., 2010) were conjugated to a tetrameric polyamidoamine scaffold (PAMAM) to generate oligomers "PAMAM-GD2" and "PAMAM-GD3," which are lipid-free, water soluble, and maintain the native structure found in native GD2 or GD3 ganglioside carbohydrates (Tong et al., 2010).

The PAMAM-GD2 and PAMAM-GD3 used as vaccines are highly immunogenic and elicit humoral responses that are selectively cross-reactive with GD2 or GD3 on the tumor cell surface. While anti-ganglioside humoral immunity is a helpful biomarker and may be therapeutically relevant, it was not absolutely required. Rather, cellular immunity elicited by the vaccine is more relevant to cancer therapy. Direct vaccination, or adoptive transfer of T cells purified from vaccinated donors, results in tumor-infiltrating lymphocytes (TILs) of the TCR$\gamma\delta$ phenotype and the $CD8^+$ phenotype, and a high therapeutic index in four aggressive and metastatic syngeneic tumor models. The vaccine is also effective in prophylactic paradigms. These principles can be expanded to other high-value targets of the TMG family (comprising >20 members), as well as to other carbohydrates expressed in a significant number of cancers.

RESULTS

Design and Synthesis of Precursor Carbohydrate Analogs, and Dendrimer Vaccine Products

The carbohydrates of normal gangliosides and TMGs share common structures. For example, GD2 and GD3 differ from each other by one sugar (Figure S1A), and the ubiquitously expressed GM1 differs from GD2 by two sugar units. Hence, it is very difficult to safely raise anti-ganglioside immunity. We prepared ganglioside mimetics that are structurally identical to native GD2 and GD3 carbohydrates and without the variable lipid tail, to reduce heterogeneity and the risk of cross-reactivity. Synthetic analogs *p*-amino phenyl ether-GD2 (AP-GD2) and *p*-amino phenyl ether-GD3 (AP-GD3) were generated, whereby their amine group can be exploited for conjugation to amenable scaffolds (Figure S1B) (Tong et al., 2010).

In AP-GD2 and AP-GD3, the anomeric center of the glucose linked to the phenyl ether is in the β-configuration, which is the native linkage found between sugar and ceramide in the natural gangliosides. This stereochemistry is key for preserving the native structure, and contrasts with some chemistry-only based synthetic methods that result in a mixture of α- and β-configurations. After high-performance liquid chromatography purification, the identity of AP-GD2 was verified by liquid chromatography-mass spectrometry, and the configuration was confirmed using ^{1}H nuclear magnetic resonance (NMR) spectroscopy, as we reported (Tong et al., 2010). The AP-GD3 was characterized similarly (data not shown). Using AP-GD2 and AP-GD3 glycomimetic precursors, we synthesized lipid-free, water-soluble oligomeric products to be used as vaccines.

Purified AP-GD2 and AP-GD3 were converted to the corresponding isothiocyanate and coupled to the free amines of PAMAM G0 dendritic core to provide the corresponding thioureas, PAMAM-GD2 and PAMAM-GD3 (Figure S1C). After separation from unreacted precursors and excess reagents, PAMAM-GD2 and PAMAM-GD3 were characterized using thin-layer chromatography, NMR spectroscopy, and quantitative ELISA (see STAR Methods and Figures S2A–S2E, S3A, and S3B).

Vaccines Elicit Humoral Immunity Selective against GD2 and GD3

The immunogenicity of PAMAM-GD2 and PAMAM-GD3 antigens was tested *in vivo*, using humoral immunity as a biomarker. After two injections with vaccine (at days −10, and −4), the sera were collected (at day 0) for testing by flow-cytometry binding to native gangliosides on the tumor cell surface, and testing by ELISA binding to AP-GD2 or AP-GD3 precursors, and to PAMAM-GD2 or PAMAM-GD3 vaccine products, or to native gangliosides.

Flow cytometry showed that test antisera bound to the surfaces of EL4-$GD2^+$ and EL4-$GD3^+$ cells. Negative control sera (pre-immune or PBS-vehicle-injected mice) exhibited background reactivity. In cellular controls, the test antisera did not

bind to Jurkat cells, which are GD2$^-$ and GD3$^-$ but express other gangliosides including GM1, indicating that antisera are GD2- or GD3-specific. Representative data for two PAMAM-GD2 vaccinated mice (M1 and M3) are shown in Figure 1A. These data indicate that the resulting humoral immunity cross-reacts with native ganglioside on tumor cells. Similar assays with antisera from PAMAM-GD3-immunized mice resulted in similar conclusions (data not shown).

ELISA measured antisera binding to vaccine precursor AP-GD2, or PAMAM-GD2 vaccine immobilized on plates, and further confirmed that vaccination raises antibodies against the immunogen (Figure 1B) as well as to native GD2 or native GD3 immobilized on plates (Figure S4). ELISA using antisera from PAMAM-GD3-immunized mice resulted in similar conclusions (data not shown). The test antisera from PAMAM-GD2 vaccinated mice had some degree of cross-reactivity with GD3 (and test antisera from PAMAM-GD3 vaccinated mice had some degree of cross-reactivity with GD2). This was not surprising because GD2 and GD3 share a common carbohydrate core (see Figure S1A).

In both the flow cytometry and the ELISA studies, the use of anti-immunoglobulin G (IgG)-specific secondary reagents indicates that the humoral response can mature and class-switch. The ELISA and FACScan results were consistent with each other, and immunization generated responses in 57 out of 60 mice tested (95%). It is noteworthy that vaccination used relatively low doses of antigen (50–100 μg/dose), and that titers increased after the second vaccination (see Figure S4).

As further validation that vaccination activates humoral immunity, hybridomas were prepared using B cells from vaccinated mice. The fusion generated several distinct anti-GD2 or anti-GD3 mAbs (W.T., R.R., F.B., and H.U.S., unpublished data).

While a mature humoral response may be therapeutically useful, and it is a convenient biomarker of vaccine immunogenicity, we next focused on cellular immunity.

PAMAM-GD2 Vaccination Expands T Cells that *Ex Vivo* Are Cytotoxic to GD2$^+$ Target Cells

The proliferation of lymph node and spleen primary T cells collected from naive mice or PAMAM-GD2 vaccinated mice was studied by measuring proliferation *in vitro* in response to stimulation by EL4-GD2$^+$ target cells or control Jurkat cells (Figure 2).

T cells from vaccinated mice proliferated when challenged with mitomycin-treated EL4-GD2$^+$ cells, but not when challenged with mitomycin-treated control Jurkat cells. T cells from non-vaccinated mice did not proliferate when challenged with either mitomycin-treated cell type. Mitomycin-treated EL4-GD2$^+$ and Jurkat cells did not incorporate [^{3}H]thymidine (188 ± 4 cpm and 107 ± 5 cpm, respectively) (Figure 2A). In cell-viability controls, treatment with concanavalin A (ConA) stimulated T cell proliferation in vaccinated and non-vaccinated mice to a similar degree (21,457 ± 504 cpm and 19,834 ± 309 cpm, respectively). These controls demonstrate that DNA synthesis takes place in the T cells from vaccinated mice when challenged with cells expressing GD2$^+$.

Similar proliferation results were obtained by vital dye cell counting. T cells from vaccinated mice (1:40 target-to-effector ratio) increased in number after co-culture with live EL4-GD2$^+$ target cells but did not increase in control co-cultures with live Jurkat cells (Figure 2B). After 7 days of co-culture all the EL4-GD2$^+$ cells were dead but Jurkat cells were alive (see morphology in Figure 2C). These data demonstrate that T cells from vaccinated mice can be selectively cytotoxic to GD2$^+$ tumor cells.

PAMAM-GD2 Vaccination Is Therapeutic against Metastatic GD2$^+$ Tumors

We studied PAMAM-GD2 as a vaccine *in vivo*. In a tumor-prophylactic paradigm, immune-competent C57/Bl6 mice were vaccinated twice (at days −9 and −3) prior to tumor implantation, followed by subcutaneous inoculation of EL4-GD2$^+$ cells (at day 0). In a tumor-therapeutic paradigm, mice were inoculated subcutaneously with EL4-GD2$^+$ cells (at day 0), followed by vaccination at days 3 and 7 post implantation (Figure 3A). EL4-GD2$^+$ cells are syngeneic, grow very aggressively, and are palpable at day 3 post inoculation (i.e., the day of first vaccination in the therapeutic model), and are highly metastatic to lymph nodes.

Vaccinated mice had significantly smaller primary tumors than control mice, in the prophylactic and the therapeutic paradigms (Figure 3B). Prophylactic and therapeutic experiments with PAMAM-GD2 vaccination were reproduced four times independently. Standardizing the primary tumor volumes of vehicle-injected control mice in each experiment to 100%, the vaccination reduced primary tumors by a significant ∼50% at the endpoint (Figure 3C).

Adoptive Transfer of T Cells from Vaccinated Donors Protects Tumor-Bearing Recipient Mice

We tested whether adoptive transfer of T cells would convey immune protection against tumors. A dose-escalation study (Figure S5) showed that the adoptive transfer of 4 × 10^6 T cells collected from vaccinated donor mice was sufficient to convey an effective anti-tumor response in a therapeutic paradigm (adoptive transfer was done at day 3 post tumor inoculation). This dose was selected for further experiments.

Mice bearing subcutaneous EL4-GD2$^+$ tumors received an adoptive transfer of 4 × 10^6 T cells obtained from PAMAM-GD2 vaccinated donor mice or were untreated as control. The recipient group had significantly smaller primary tumors compared with the control group (n = 5 per group) at all days measured (respectively, ∼500 mm^3 versus ∼1,200 mm^3 at day 14) (Figure 3D). Importantly, the recipient group had no significant metastasis to the lymph nodes, which is the major site of metastasis. The control group had lymph nodes ∼10-fold heavier than naive healthy mice, while the recipient group was significantly smaller and similar to naive healthy mice (Figure 3E, representative pictures at day 14 post tumor implantation are shown as an inset).

PAMAM-GD3 Vaccination Is Therapeutic against Metastatic GD3$^+$ Tumors

In a therapeutic paradigm, mice bearing subcutaneous EL4-GD3$^+$ tumors (n = 8 per group) were untreated (control), or vaccinated, or received adoptive transfer of 4 × 10^6 T cells purified from donor mice that had been vaccinated. Both

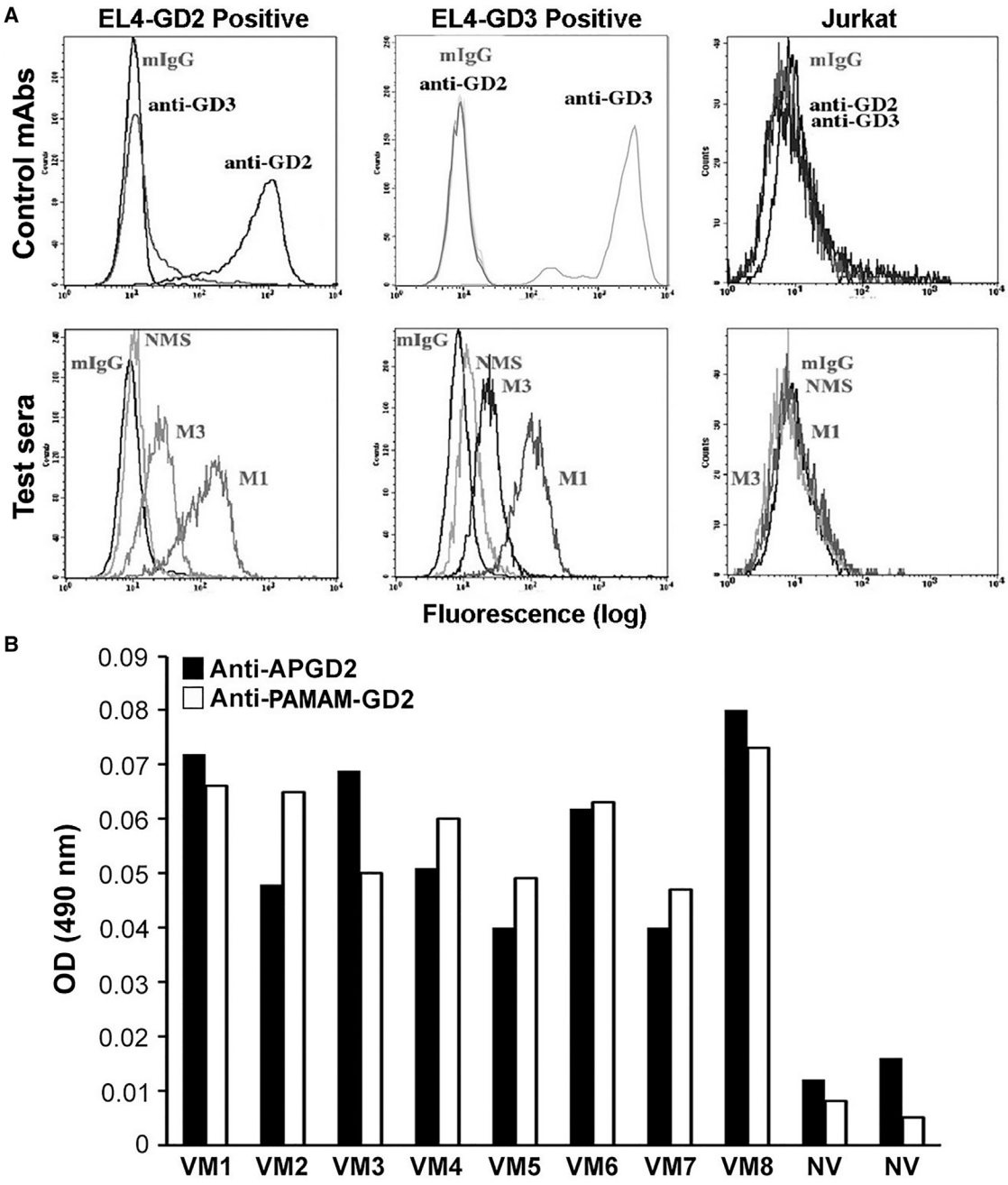

Figure 1. Vaccination with PAMAM-GD2 Elicits Humoral Immunity

Mice vaccinated with PAMAM-GD2 (shown) or PAMAM-GD3 (not shown) developed antisera to native GD2 or GD3 (53/56 mice, 95%). Antisera binds to GD2 tumor cell surfaces in flow-cytometry studies, and binds to AP-GD2 precursor or PAMAM-GD2 in ELISA studies. Antisera binding to a panel of native gangliosides is shown in Figures S3 and S4.

(A) Representative flow cytometry for PAMAM-GD2-vaccinated mouse 1 (M1) and mouse 3 (M3) producing anti-GD2 antibodies of the IgG class, compared with negative controls. Cellular controls Jurkat and EL4-GD3^{+} cells show that the antisera had no reactivity to other gangliosides other than to the structurally related GD3. mAbs directed to GD2 or GD3 are used as positive controls (top panels).

(B) Sera from mice vaccinated (VM) with PAMAM-GD2 (n = 8) or non-vaccinated (NV) controls (n = 2) were tested in ELISA for binding to immobilized AP-GD2 precursor (which is PAMAM-free, black bars), or immobilized PAMAM-GD2 vaccine (white bars). Each ELISA for each test sera were studied in triplicate at least twice independently. The serum dilution used was 1:50. The optical density (OD) values shown are after background correction, done by subtracting the OD of wells where there was no immobilized GD2, or wells with immobilized GM1 (these controls are not different from each other).

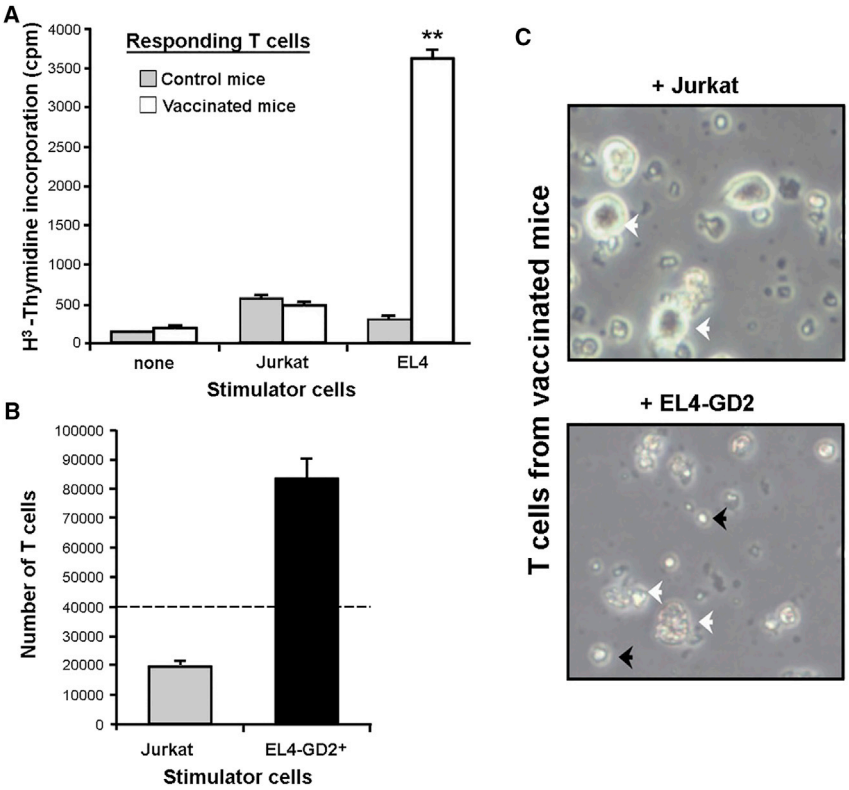

Figure 2. Vaccination with PAMAM-GD2 Affords T Cell Proliferation in a Target-Selective Manner after Challenge *Ex Vivo*

(A) T cells from vaccinated or naive mice were cultured with mitomycin-treated tumor cells (1:10 target-to-effector ratio). T cell proliferation was evaluated in [^{3}H]thymidine incorporation assays (mitomycin-treated tumors do not proliferate). EL4-GD2$^+$ cells stimulate T cells from vaccinated mice but control Jurkat cells lacking GD2 do not. T cells from unvaccinated naive mice do not proliferate to either challenge. ConA was used as positive control. Mitomycin-treated EL4-GD2$^+$ or Jurkat cells do not proliferate and only act as stimulators. Data are mean ± SD (n = 4) and are analyzed by Student's t test. **$p < 0.01$. Representative of two independent experiments, each in quadruplicate.

(B) T cell proliferation was measured by trypan blue exclusion. Purified T cells from PAMAM-GD2 vaccinated mice (~40,000/well) were seeded with live EL4-GD2$^+$ (black bars) or live Jurkat (gray bars) stimulator cells (1,000/well) (1:40 target-to-effector ratio). After 7 days *in vitro*, the T cells challenged by EL4-GD2$^+$ proliferated significantly to ~80,000 whereas control cultures decreased form ~40,000 input to ~20,000 (n = 6 replicate wells).

(C) After 7 days *in vitro*, all the Jurkat cells were alive and proliferating; while the EL4-GD2$^+$ cells were dead (white arrowheads), and the dishes contained cells with the morphology of activated or blasting T cells (black arrowheads).

treatments significantly delayed primary tumor growth, at all days measured, compared with controls (Figure 4A). Therapeutic experiments were reproduced three times independently. Standardizing the primary tumor volumes of control mice in each experiment to 100%, vaccination reduced primary tumors by a significant ~40% at the endpoint (Figure 4B). The vaccination and the adoptive transfer also significantly reduced EL4-GD3$^+$ metastasis to the lymph nodes (Figure 4C, representative pictures of the lymph nodes are shown as an inset). This is biologically significant, as preventing metastasis is a key parameter for therapeutic efficacy.

Two additional metastatic GD3$^+$ tumor models were evaluated, the B16 melanoma (Figure 4D) and the LLC1 lung cancer (Figure S6). The PAMAM-GD3 vaccine proved effective for both. The B16-GD3$^+$ melanoma is inoculated intravenously and does not produce a primary tumor. Lung metastases can be quantified as melanin-containing black nodules. Mice bearing B16-GD3$^+$ tumors were a control group (n = 9), or at days 3 and 8 post tumor inoculation they were vaccinated with PAMAM-GD3 (n = 12). In this therapeutic paradigm the vaccinated mice had ~60 black spots per lung (most of relatively small size) compared with control mice with ~210 black spots per lung (most of relatively larger size) (Figure 4D).

Similar data were obtained when using the LLC1-2E5 line that expresses GD2 and GD3. Subcutaneous injection of LLC1-2E5 cells forms a primary tumor that metastasizes to lung, forming white nodules. In a therapeutic paradigm, PAMAM-GD3 vaccination resulted in the absence or the significant reduction of LLC1-2E5 lung nodules (Figure S6).

PAMAM-GD2 and PAMAM-GD3 Vaccination Extends Life Span

Additional therapeutic studies and Kaplan-Meier survival plots were done using the subcutaneous EL4-GD2$^+$ and EL4-GD3$^+$ models. Vaccinated groups had significantly prolonged survival (Figures 5A and 5B) with PAMAM-GD2 vaccine ($p < 0.002$) and PAMAM-GD3 vaccine ($p < 0.0005$) compared with the respective control groups.

In addition, the PAMAM-GD2 vaccinated mice had axillary lymph nodes of 53% lower weight ($p < 0.005$, non-paired two-tailed t test), and the PAMAM-GD3 vaccinated mice had axillary lymph nodes of 37% lower weight ($p < 0.05$, non-paired two-tailed t test), indicating reduced metastases.

The terminal endpoint was defined as death or as a primary tumor volume >1,100 mm^3. Compared with their respective control groups the vaccinated groups had significantly smaller primary tumors, with results similar to the tumor volume data reported in Figure 3. Given that the lymph nodes were collected at different endpoints (e.g., in the EL4-GD2$^+$ model at days 16–19 for control; and at days 18–21 for vaccinated) the reduced metastasis may not be directly related to primary tumor size, but rather may be associated with a protective systemic immunity.

Together, these data indicate that vaccination is effective at reducing primary tumors, at reducing metastasis, and at extending survival.

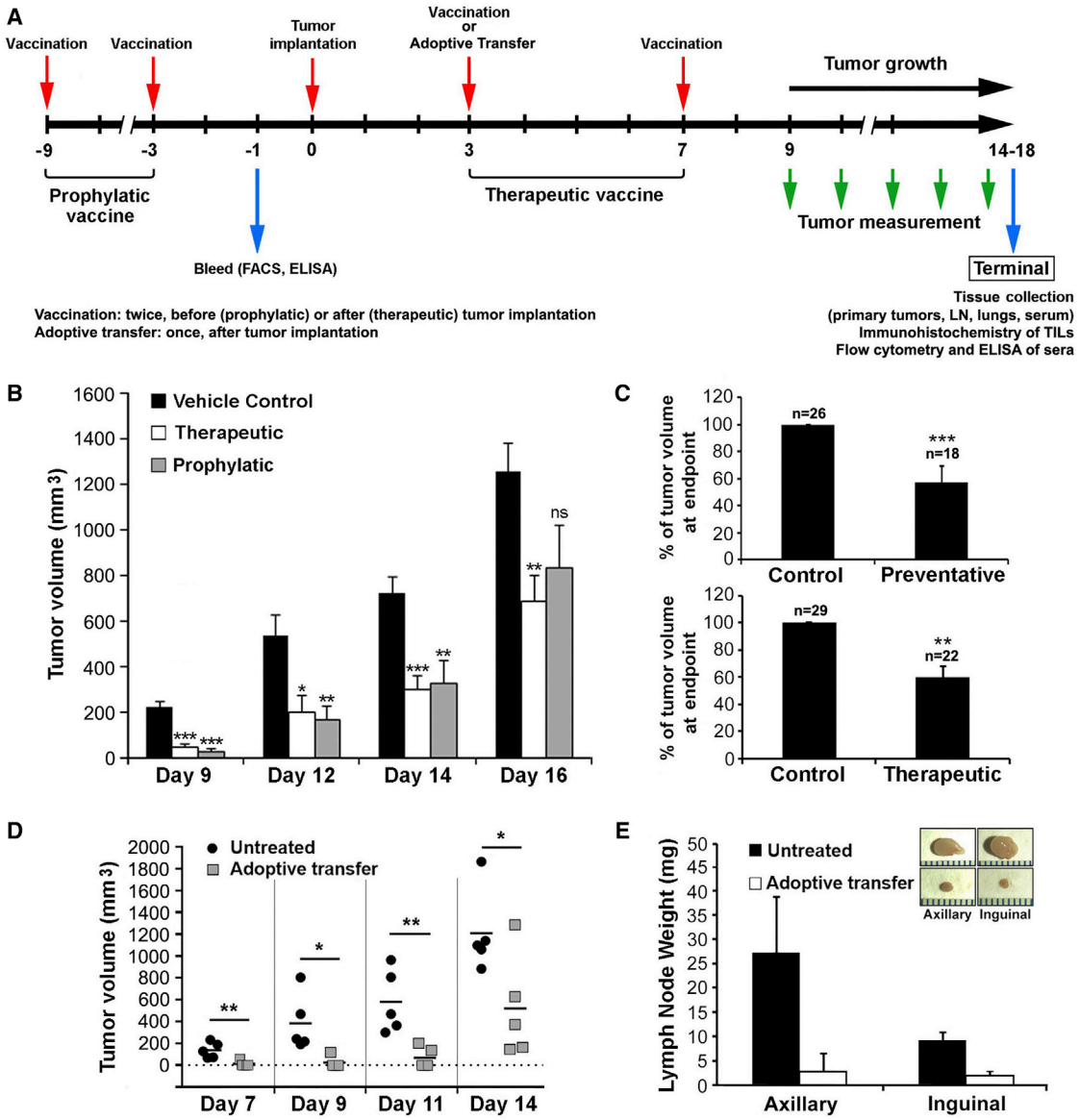

Figure 3. PAMAM-GD2 Provides Protection from EL4-GD2$^+$ Tumors through Vaccination or Adoptive T Cell Transfer

(A) Flowchart of *in vivo* vaccinations and experimental endpoints (prophylactic or therapeutic, and therapeutic adoptive transfers).

(B) Representative experiments against EL4-GD2$^+$ tumors. In the vaccine group there was one mouse with no primary tumor at day 15 and another at day 18. "Complete regressions" were not considered for the graph shown, to exclude the unlikely possibility of failure of tumor implantation. * $p < 0.05$, ** $p < 0.01$, *** $p < 0.001$.

(C) Average primary tumor volumes ± SD for four independent prophylactic experiments and four independent therapeutic experiments. Data were standardized to control mice as 100% at endpoint, and analyzed by two-tailed t tests. **$p < 0.01$ and ***$p < 0.001$.

(D) The adoptive transfer (AT) therapy group (n = 6) had significantly delayed primary tumor growth compared with control (n = 6) at all days measured. *$p < 0.05$ and **$p < 0.01$.

(E) Quantification of metastasis by measuring lymph node weights. Mice bearing tumors (n = 6) have ~10-fold heavier lymph nodes than naive mice not bearing tumors. Mice bearing tumors (n = 6) but receiving AT of T cells had relatively normal-sized lymph nodes. Representative pictures are shown as an inset.

Vaccination of Tumor-Free Mice Induce Expansion of TCRγδ T Cells

To study the cellular immunity mechanism in more detail, tumor-free mice were left untreated (control group, n = 2) or vaccinated with PAMAM-GD2 (vaccine group, n = 3). Following verification of a humoral response (as a biomarker of vaccination, by flow cytometry and ELISA testing of sera, as in Figure 1), the T cells were collected from lymph node and spleen and immediately purified using a negative selection kit. Live single cell suspensions were immediately phenotyped by flow cytometry.

In both tumor-free groups nearly 100% of the purified cells were CD3$^+$, but it is noteworthy that in the vaccinated

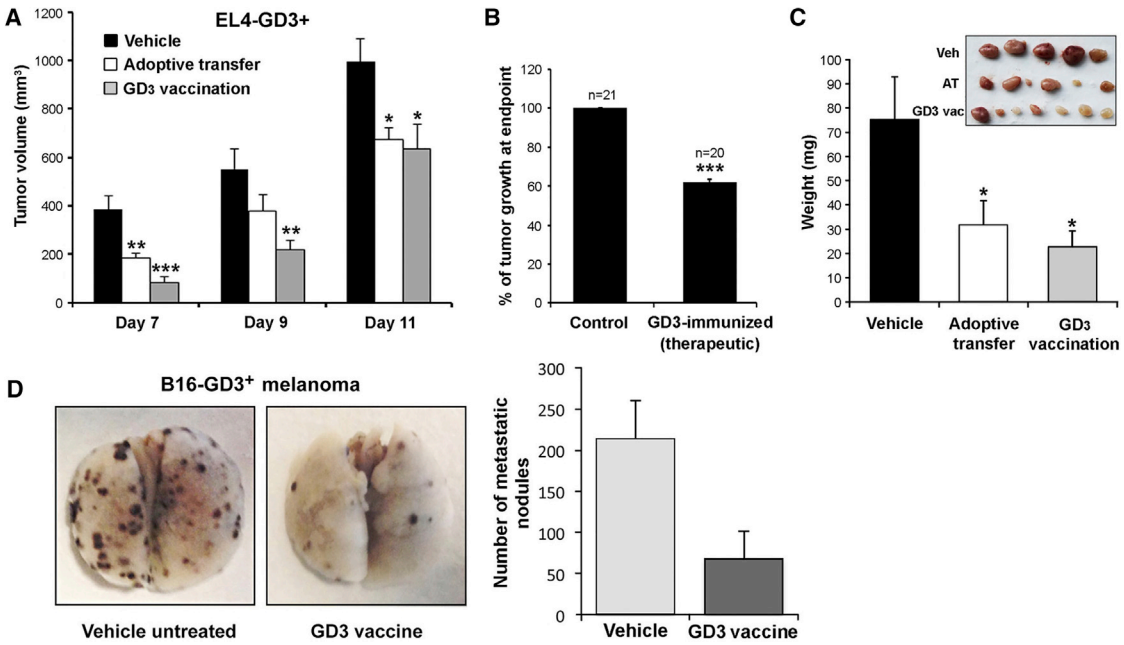

Figure 4. PAMAM-GD3 Provides Protection from Tumors through Vaccination or Adoptive T Cell Transfer

(A) Mice bearing subcutaneous EL4-GD3$^+$ tumors were randomized into groups: control (n = 8), vaccinated with PAMAM-GD3 (n = 8), or adoptively transferred with T cells from vaccinated mice (n = 8). The adoptively transferred and the vaccinated groups displayed significantly delayed primary tumor growth compared with control at all days measured. Shown are average primary tumor volumes ± SD. * $p < 0.05$, ** $p < 0.01$, *** $p < 0.001$.

(B) Average primary tumor volumes ± SD for three independent therapeutic experiments. Data were standardized to control mice as 100% at endpoint, and analyzed by two-tailed t tests. ***$p < 0.001$.

(C) Quantification of metastasis by measuring lymph node weights. Control tumor-bearing mice have larger lymph nodes than tumor-bearing mice that received adoptive transfer (AT) of T cells or PAMAM-GD3 vaccination (n = 8 each group). Representative pictures are shown as an inset.

(D) PAMAM-GD3 vaccine reduces lung metastasis of B16-GD3$^+$ melanoma cells. Cells were injected in the tail vein (n = 21, day 0), after 3 days mice were randomized and either vaccinated (50 μg/mouse intraperitoneally, n = 12) or used as control (n = 9). Mice were sacrificed at day 17, and metastatic nodules were counted. Histogram shows the average number of metastatic nodules ± SD. All control mice had ~4-fold more nodules of larger size than the vaccinated mice. Representative lungs are shown.

group ~30% of the cells had significantly increased CD3 density (CD3^{hi}) compared with the untreated control group (Figure 6A). Moreover, compared with the untreated control group the vaccinated group had an increased percentage of the TCRγδ subset of T cells (Figure 6B), which increased from 3% to 5% in control mice to 8%–11% in vaccinated mice.

Vaccination of Tumor-Bearing Mice Induces Expansion of TCRγδ T Cells and CD8$^+$ T Cells

Phenotyping studies were then carried out with purified cells obtained from mice bearing subcutaneous LLC1-2E5 tumors. Tumor-bearing mice were untreated (control group) or vaccinated with PAMAM-GD3 (vaccine group), and single cell suspensions were purified as above and phenotyped by flow cytometry for CD3, CD4, CD8, CD25, TCRβ, TCRγδ, and FOXP3 markers.

In tumor-bearing mice, group comparisons show that in the vaccine group there is an unexpected increase in the percentage of CD8$^+$CD3$^+$ T cells relative to CD4$^+$CD3$^+$ T cells (Figure 6C). In the tumor-bearing untreated mice the CD4/CD8 ratio is 1:1. This 1:1 ratio is different from the 2:1 ratio of naive normal mice (tumor-free, untreated), suggesting that the presence of tumor causes a CD8$^+$ expansion. In the tumor-bearing vaccinated mice the CD4/CD8 ratio changes further to 1:2, suggesting that vaccination causes a further CD8$^+$ expansion but only when a tumor is present.

In tumor-bearing mice, similar to what we report above for tumor-free mice, in the vaccine group there is an increase in the percentage of γδ TCR CD3$^+$ cells relative to TCRβ$^+$ CD3$^+$ cells (Figure 6D) compared with the control group. This similar increase in γδ TCR cells in vaccinated mice (whether or not mice bear tumors) suggests that the γδ T cell expansion may be due solely to the vaccination.

Together, these data suggest that the presence of a tumor activates a CD8$^+$ immune response, which is likely recognizing peptide antigens from the tumor but which is ineffective at protecting the host. Vaccination with a glycomimetic elicits a γδ TCR expansion (in tumor-free and in tumor-bearing mice); and in tumor-bearing mice vaccination elicits a subsequent additional anti-tumor CD8$^+$ T cell expansion, which makes the immune response more effective at protecting the host.

Regarding other markers studied, vaccination of LLC1-2E5 tumor-bearing mice did not significantly alter the total number of CD4$^+$ regulatory T cells expressing CD25$^+$FoxP3$^+$ (T regulatory cells), or CD3$^+$ T cells expressing TCRβ (data not shown).

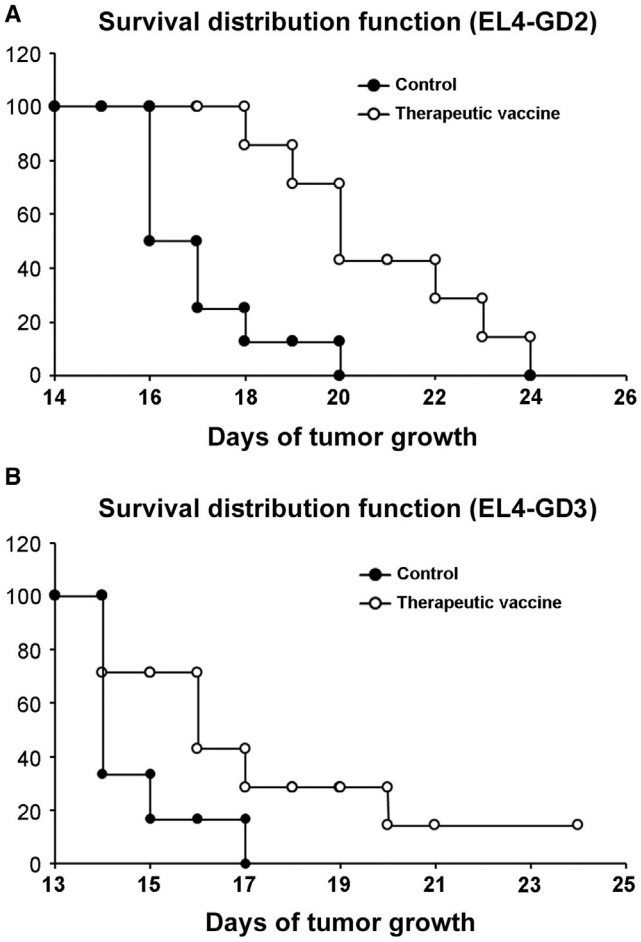

Figure 5. Therapeutic Vaccination Prolongs Survival in EL4 Tumor-Bearing Mice

After subcutaneous implantation of tumors, mice were divided into untreated or vaccinated groups (n = 7–8 per group). The vaccinated groups (A) PAMAM-GD2 or (B) PAMAM-GD3 had significantly prolonged survival versus the corresponding control ($p < 0.001$ for PAMAM-GD2 and $p < 0.0005$ for PAMAM-GD3; paired, two-tailed Student's t test). A long-term surviving mouse (>35 days) had a measurable primary tumor that regressed over time. In addition, vaccinated groups had reduced metastases to lymph nodes (see text).

PAMAM-GD3 and PAMAM-GD2 Vaccines Induce Expansion of TCRγδ T Cells and CD8$^+$ T Cells that Infiltrate Tumors

To study the function of the expanded T cells, mice bearing subcutaneous LLC1-2E5 tumors were left untreated (control group) or received adoptive transfer (AT) of T cells purified from PAMAM-GD3-vaccinated mice (recipient group). Immunohistochemistry of tumor cryosections showed the presence of TCRγδ TILs in the AT group (Figure 7A).

Increasing the number of adoptively transferred T cells positively correlated with increasing numbers of TCRγδ TILs, while in the control group not recipient of AT (no AT) the TCRγδ TILs were undetectable (Figure 7B).

Similar immunohistochemical studies were done in tumor cryosections prepared from mice bearing EL4-GD2$^+$ tumors. The recipient group (receiving AT of T cells from donor mice vaccinated with PAMAM-GD2) had a significantly higher number of CD8$^+$ TILs. Moreover, after AT the number of CD4$^+$ TILs increases on average but the data are not statistically significant due to low numbers and variability. The control group (not receiving AT) had low or no detectable CD8$^+$ or CD4$^+$ TILs (Figure 7C). Note that the EL4-GD2$^+$ lymphoma is CD3$^+$ and TCRαβ$^+$, but does not express CD4 or CD8 detectable by flow cytometry. Hence the increased immunostaining in the tumor cryosections is due only to immune cell infiltration.

Hypervaccination with PAMAM-GD3 Does Not Elicit Detectable Negative Side Effects

Potential negative side effects were evaluated in mice (n = 4 per group) that were injected with saline as control, or hyperimmunized with PAMAM-GD3 (5 intraperitoneal vaccinations: 3 × 100 μg and 2 × 50 μg, each ~14 days apart, over a 56-day period).

At day 60 after first injection, blood profiles, enzymes associated with liver or kidney damage, motility, vision and retinal health, wire grip strength, and learning and memory were quantified, and behavior associated with pain was monitored. All parameters tested were normal and equal for both groups. Data for the Morris Water Maze test (Figure S7) shows that the performance of hyperimmunized and control groups was indistinguishable with respect to swimming and motility (Figure S7A), learning (Figure S7B), and memory recall (Figure S7C). Together, these data indicate that PAMAM-GD3 vaccination (even hypervaccination) was free of negative side effects known to burden passive administration of anti-ganglioside mAbs in humans and rodents (Navid et al., 2010).

DISCUSSION

TMGs as Cancer Drivers and Valuable Cancer Targets

Gangliosides such as GD2 and GD3 are TMGs expressed at high levels in cancer (Daniotti et al., 2013, 2016; Gagnon and Saragovi, 2002), and are etiological for cancer (Aixinjueluo et al., 2005; Cazet et al., 2009; Furukawa et al., 2006; Gagnon and Saragovi, 2002; Hamamura et al., 2011; Iwabuchi et al., 2000; Liu et al., 2006; Nakashima et al., 2007; Shibuya et al., 2012; Todeschini et al., 2007; Tong et al., 2015; Yoshida et al., 2002; Ziche et al., 1992) and immune evasion or suppression (Caldwell et al., 2003; Gagnon and Saragovi, 2002; Shurin et al., 2001; Yoshida et al., 2001). These valuable markers, comprising >20 glycosphingolipids, would be ideal targets for immune-mediated therapy.

Cell Immunity and Carbohydrates

Carbohydrate dendrimers of GD2 and GD3 mimetics that possess native-like β-linkages at the reducing end are highly immunogenic. The products act as vaccines to activate an innate cellular immunity that *ex vivo* and *in vivo* is selectively cytotoxic against tumors expressing these TMGs.

Vaccination expands non-overlapping CD3$^+$ TCRγδ and CD3$^+$CD8$^+$ T cells. The γδ and the CD8$^+$ T cell expansion can be achieved through direct vaccination *in vivo* and the CD8$^+$ cytotoxic T cell expansion can be further promoted *ex vivo* by exposure of T cells to tumors. Direct vaccination (or AT therapy

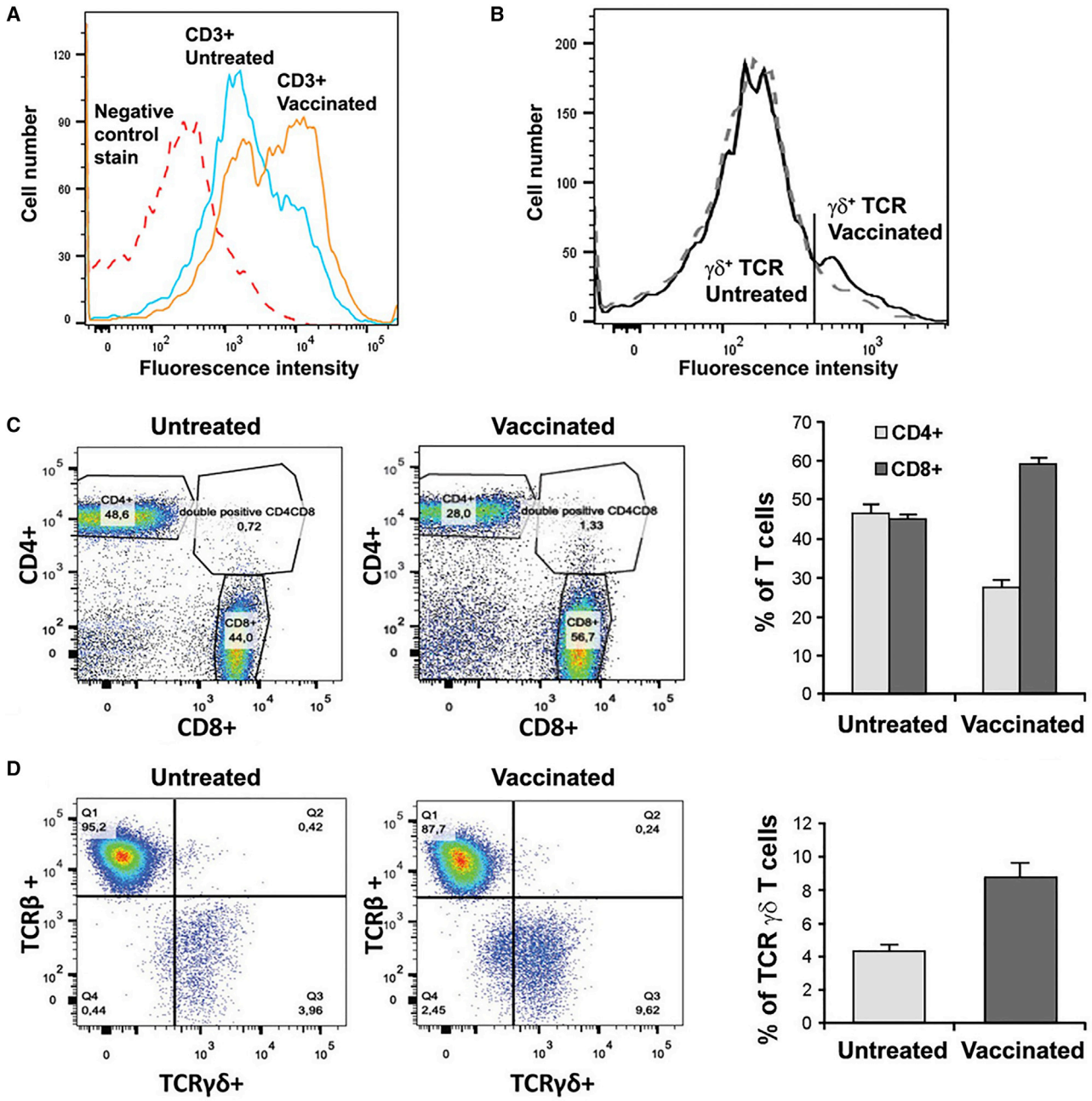

Figure 6. Phenotype of Expanding T Cells Resulting from Vaccination

Primary cells were phenotyped by flow cytometry.

(A and B) Tumor-free mice were untreated (n = 2) or were vaccinated with PAMAM-GD2 (n = 3), and cells from lymph nodes and spleen were purified using a negative selection kit that removes non-T cells including B cells, NK, and NK-T cells. (A) CD3 expression, with the negative control staining (dashed line) being identical for both. Vaccination generates a $CD3^{hi}$ population. (B) TCR γδ expression. The area to the right of the marker shows TCR γδ-expressing cells, with an additional peak in the vaccinated group (solid line) versus the untreated group (dashed line). The negative control staining, not shown for clarity, overlays the histogram to the left of the marker.

(C and D) Mice bearing subcutaneous LLC1-2E5 tumors were untreated or vaccinated with PAMAM-GD3 (n = 4 per group), and their T cells were purified as above. Flow cytometry was gated on live $CD3^+$ cells. (C) Vaccination of tumor-bearing mice elicits expansion of the $CD8^+$ relative to $CD4^+$ T cells, as shown by the bar graph (quantification ± SD). In the untreated tumor-bearing mice the CD4/CD8 ratio is 1:1, and the ratio changes to 1:2 in the vaccinated tumor-bearing mice. (D) Vaccination of tumor-bearing mice elicits expansion of the $TCR\gamma\delta^+$ relative to $TCR\alpha\beta^+$ T cells, as shown by the bar graph (quantification ± SD).

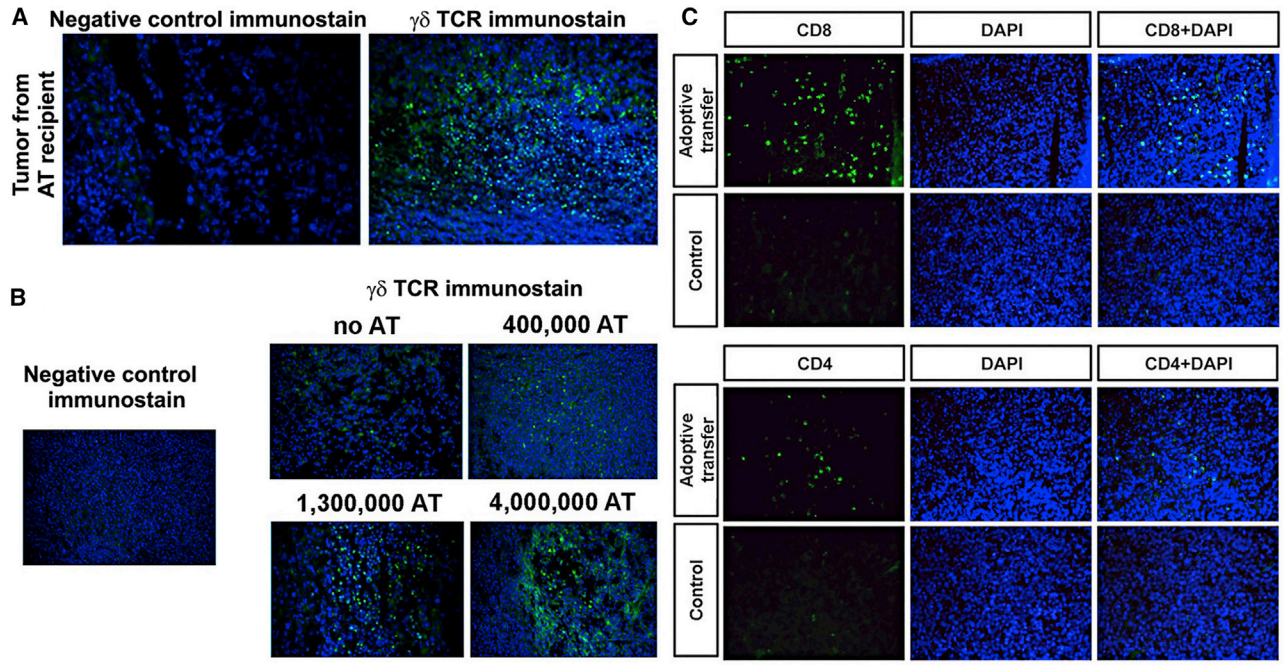

Figure 7. Adoptive Transfer of T Cells from Vaccinated Donors Results in TILs

(A and B) Mice bearing subcutaneous LLC1-2E5 tumors received adoptive transfer (AT) of T cells purified from PAMAM-GD3-vaccinated donors. Tumor cryosections were immunostained for TCRγδ using two different Abs, yielding consistent data (clone GL3 eBioscience cat. #14-5711-82, shown, and clone UC7-13D5, not shown). (A) shows the presence of γδ TCR TILs after adoptive transfer. (B) shows that an AT dose escalation yields increasing γδ TCR TILs (0, 0.4 × 10^6, 1.3 × 10^6, or 4 × 10^6 transferred T cells). Negative control stain is species- and isotype-matched irrelevant primary Ab.

(C) Mice bearing subcutaneous EL4-GD2$^+$ tumors received AT of T cells purified from untreated or PAMAM-GD2 vaccinated donor mice. Cryosections were immunostained for CD8 or CD4, and co-stained with DAPI. Compared with the control untreated group, the AT group had increased CD8$^+$ TILs. There are small increases in CD4$^+$ TILs but due to low numbers the data are not significant.

All micrographs taken at 20× magnification.

of T cells generated through vaccination) results in TCRγδ and CD8$^+$ TILs, indicating that these cells target the tumor mass.

In therapeutic paradigms the treatments were safe and effective, prevented tumor growth and metastasis, and extended survival in four very aggressive syngeneic cancer models. This is proof of concept that a synthetic small-molecule glycomimetic with no carrier protein can be used as a therapeutic cancer vaccine; and endorses the theory that other tumor gangliosides and carbohydrate vaccines should also be equally tested.

TCRγδ T Cells and Carbohydrates

A small percentage of T cells express γδ TCRs that recognize (phospho)lipid antigens. The γδ T cells span definitions of both innate and adaptive immune responses because they carry out effector, helper, and adjuvant-like functions by interacting with macrophages, dendritic cells, NK cells, T cells, and B cells (Bonneville et al., 2010; Van Rhijn et al., 2016; Vantourout and Hayday, 2013). While γδ T cells are not self-MHC-restricted, they can distinguish "foreign" or transformed cells, and can elicit memory (Hoft et al., 1998; Huang et al., 2015; Sheridan et al., 2013). For these reasons γδ T cells have been utilized for cancer therapy (Dieli et al., 2007; Khan et al., 2014).

Our study reveals the unexpected expansion of γδ T cells being driven by a pure carbohydrate dendrimer, rather than lipids or (glyco)lipids or (glyco)peptides. In terms of kinetics, the PAMAM-glycan vaccine appears to induce an initial γδ T cell response that circumvents tumor-mediated immunosuppression or immune-checkpoint blockade and later initiates a cascade of immune responses including CD8$^+$ T cells. The γδ T cell expansion occurs rapidly after vaccination in mice independent of tumor presence, and expansion of the CD8$^+$ T cells occurs subsequent to tumor challenge *in vivo* or *ex vivo*. Other agents such as aminobiphosphonates (alendronate and analogs) also expand γδ T cells, but do so in an antigen-non-specific manner and through different mechanisms.

We hypothesize that vaccination induces γδ T cells, which subsequent to tumor challenge recruit or help to expand the CD8$^+$ T cells. The γδ T cells thus may have acted as antigen-presenting cells (APCs) to induce the proliferation and activation of antigen-specific CD8$^+$ αβ effector T cells, as reported in other models (Brandes et al., 2009; Paul and Lal, 2016). While a low percentage of γδ T cells can acquire the CD8$^+$ phenotype and act as MHC-unrestricted cytotoxic effector T cells (Morita et al., 1991), the majority of the expanded CD8$^+$ TILs in our *in vivo* work are most likely of the αβ TCR phenotype, given that they exceed the total number of γδ T cells.

Further characterization of the kinetics and the mechanisms are ongoing based on the hypothesis that CD8$^+$ T cell expansion may be due to antigen migration and recognition of protein targets—rather than gangliosides—when an initial anti-tumor

immune response induces T-cell-mediated destruction of tumor cells (e.g., from a therapeutic anti-cancer vaccine or from immune-checkpoint blockade), with subsequent presentation of additional tumor-associated secondary antigens (Efremova et al., 2017; Gulley et al., 2017; Ott et al., 2017).

The Role of Humoral Immunity after Vaccination

In our work, a humoral response was useful as a convenient biomarker of vaccine immunogenicity, but does not seem to be absolutely required for therapy (based on adoptive T cell transfer experiments). Nonetheless a humoral response may potentiate the cellular response.

As stated, the γδ T cells are CD1 restricted (Brigl and Brenner, 2004; Park et al., 2008; Van Rhijn et al., 2016). Interestingly, GD3 has relatively high affinity for CD1d (Caldwell et al., 2003). Activation of natural killer T (NKT) cells is prevented by direct GD3-CD1 binding (Wu et al., 2003) as well as binding by other glycosphingolipids (Sriram et al., 2002). The vaccine-induced antibodies may release TMG-CD1 inhibition or mop up shed TMGs reducing TMG-CD1 binding, thus allowing γδ T cell activation. Antibodies may also improve immune responses through ADCC.

Indeed, we have used the vaccines for generating mAbs and to show that the humoral response is polyclonal and can mature. The mAbs and γδ TCR sequences expanding after vaccination may be cloned and used in CAR-T therapy.

Carbohydrates as Targets in Cancer, and Role of Sialic Acids

TMGs contain at least one sialic acid, with *N*-acetylneuraminic acid (Neu5Ac) being the predominant form. Sialic acids (α-2,3, α-2,6, and α-2,8) are also found in glycoproteins (e.g., siglecs) that negatively regulate the immune system much like TMGs or immune-checkpoint inhibition do. It is therefore tempting to draw a correlation. Indeed, gangliosides such as GD2 and GD3 bind to CD33-related siglecs with a certain degree of selectivity, promoting metastasis and tumor progression (Ito et al., 2001; Rapoport et al., 2003).

The concept of the Glycocode (Dube and Bertozzi, 2005; Rodriguez et al., 2018) poses that protein glycosylation (mainly sialic acids have been studied) regulates biological events that are crucial to immunity and cancer progression, beyond the PD-1 type of checkpoint inhibition. These include tumor camouflage, immunosuppression, and masking of neo-epitopes. Our work would extend this concept to the glycosylation of gangliosides, with TMGs representing a glyco-immune checkpoint. Vaccines, antibodies, small molecules, soluble glycoproteins, enzymatic cleavage of sialic acids, or soluble competitors targeting the glyco-immune checkpoint would be a promising approach to therapy (Astronomo and Burton, 2010; Dube and Bertozzi, 2005; Slovin et al., 1999).

Conclusions

Vaccination with the PAMAM glycoconjugates as monotherapy affords a significant therapeutic response. Efficacy does not absolutely depend on adjuvant treatment, does not absolutely require the humoral response, and appears to be safe and free of side effects associated with passive immunity. These properties and the efficacy of the vaccines afford a high therapeutic index.

Our proof-of-concept study demonstrates a humoral response, but also uncovers unexpected properties of γδ T cell activation by a vaccine containing a carbohydrate small-molecule antigen, with further expansion of $CD8^+$ T effector cells and generation of TILs that afford protection in four very aggressive and metastatic tumors.

While γδ T cells are susceptible to PD1-mediated inhibition (Iwasaki et al., 2011), vaccination may activate γδ T cells outside the tumor inhibitory environment (Khan et al., 2014), rendering the activated T cells less susceptible to immune-checkpoint inhibition. We are exploring immune-checkpoint inhibition in combination with vaccine or with anti-GD2 or anti-GD3 mAb passive immunotherapy, expecting improved responses because the four tumor models express high levels of PDL-1. Other studies include the γδ TCR repertoire, and understanding the mechanism (CD1-mediated? CD33-related?) of activation of the γδ T cells by the vaccine.

SIGNIFICANCE

Tumor-associated-ganglioside glycosphingolipids such as GD2 or GD3 are tumor markers and etiological for cancer, but being non-immunogenic they can only be targeted using passive immunotherapy. To generate active immunity, we synthesized dendrimers of GD2 and GD3 carbohydrate headgroup structures (lipid-free, water-soluble), products that are highly immunogenic *in vivo* and are therapeutic for cancer. The data show the unexpected finding that a carbohydrate synthetic vaccine—protein-free and lipid-free—activates T cells as well as antibody responses that are protective. This principle may be expanded and applied to target a large family of tumor-associated glycolipids expressed in a significant number of cancers.

STAR★METHODS

Detailed methods are provided in the online version of this paper and include the following:

- KEY RESOURCES TABLE
- CONTACT FOR REAGENT AND RESOURCE SHARING
- EXPERIMENTAL MODEL AND SUBJECT DETAILS
  - Mice
  - Cell Lines
- METHODS DETAILS
  - Synthesis of PAMAM-GD2 and PAMAM-GD3 Dendrimers
  - Immunization
  - Tumor-Prophylactic Studies
  - Tumor-Therapeutic Studies
  - Adoptive T Cell Transfer for Therapeutic Studies
  - Characterization of Sera
  - Proliferation and Phenotypic Assays
  - Phenotyping of Freshly Isolated Primary T Cells
  - Immunofluorescence of TILs in Tumor Cryosections
  - Evaluation of Primary Tumor Growth and Metastases
- QUANTIFICATION AND STATISTICAL ANALYSIS

SUPPLEMENTAL INFORMATION

Supplemental Information can be found online at https://doi.org/10.1016/j.chembiol.2019.03.018.

ACKNOWLEDGMENTS

We thank Gloria To, Dr. T. Barhoumi, and H. Lippiatt for assistance in ELISA assays, vaccinations, and flow-cytometry analyses. This work was supported by grants to H.U.S. from the CIHR Proof-of-Principle tier 1 (POP-1) and the GlycoNet Network of Centers of Excellence. W.T. was supported by a doctoral award from the FRQS (Quebec).

AUTHOR CONTRIBUTIONS

Conceptualization, H.U.S. and W.T.; Validation and Verification, R.C., M.M., and S.M.; Formal Analysis, W.T., M.M., A.G., S.M., F.B., and R.C.; Investigation, W.T., M.M., R.C., S.M., S.J., and I.P.; Resources, M.G. and A.-M.C.; Data Curation, A.G. and F.B.; Writing – Review & Editing, H.U.S., W.T., M.M., S.M., and R.C.; Visualization, A.G., M.M., W.T., R.C., and S.M.; Supervision, H.U.S.; Project Administration, M.M. and W.T.; Funding Acquisition, H.U.S.

DECLARATION OF INTERESTS

Patent applications on the vaccines were filed by McGill University (H.U.S. and W.T., inventors).

Received: August 2, 2018
Revised: September 19, 2018
Accepted: March 27, 2019
Published: May 16, 2019

REFERENCES

Aixinjueluo, W., Furukawa, K., Zhang, Q., Hamamura, K., Tokuda, N., Yoshida, S., Ueda, R., and Furukawa, K. (2005). Mechanisms for the apoptosis of small cell lung cancer cells induced by anti-GD2 monoclonal antibodies: roles of anoikis. J. Biol. Chem. *280*, 29828–29836.

Astronomo, R.D., and Burton, D.R. (2010). Carbohydrate vaccines: developing sweet solutions to sticky situations? Nat. Rev. Drug Discov. *9*, 308–324.

Bajorin, D.F., Chapman, P.B., Wong, G., Coit, D.G., Kunicka, J., Dimaggio, J., Cordon-Cardo, C., Urmacher, C., Dantes, L., Templeton, M.A., et al. (1990). Phase I evaluation of a combination of monoclonal antibody R24 and interleukin 2 in patients with metastatic melanoma. Cancer Res. *50*, 7490–7495.

Bleeke, M., Fest, S., Huebener, N., Landgraf, C., Schraven, B., Gaedicke, G., Volkmer, R., and Lode, H.N. (2009). Systematic amino acid substitutions improved efficiency of GD2-peptide mimotope vaccination against neuroblastoma. Eur. J. Cancer *45*, 2915–2921.

Blixt, O., Vasiliu, D., Allin, K., Jacobsen, N., Warnock, D., Razi, N., Paulson, J.C., Bernatchez, S., Gilbert, M., and Wakarchuk, W. (2005). Chemoenzymatic synthesis of 2-azidoethyl-ganglio-oligosaccharides GD3, GT3, GM2, GD2, GT2, GM1, and GD1a. Carbohydr. Res. *340*, 1963–1972.

Bonneville, M., O'Brien, R.L., and Born, W.K. (2010). Gammadelta T cell effector functions: a blend of innate programming and acquired plasticity. Nat. Rev. Immunol. *10*, 467–478.

Brandes, M., Willimann, K., Bioley, G., Levy, N., Eberl, M., Luo, M., Tampe, R., Levy, F., Romero, P., and Moser, B. (2009). Cross-presenting human gammadelta T cells induce robust CD8+ alphabeta T cell responses. Proc. Natl. Acad. Sci. U S A *106*, 2307–2312.

Brigl, M., and Brenner, M.B. (2004). CD1: antigen presentation and T cell function. Annu. Rev. Immunol. *22*, 817–890.

Caldwell, S., Heitger, A., Shen, W., Liu, Y., Taylor, B., and Ladisch, S. (2003). Mechanisms of ganglioside inhibition of APC function. J. Immunol. *171*, 1676–1683.

Cazet, A., Groux-Degroote, S., Teylaert, B., Kwon, K.M., Lehoux, S., Slomianny, C., Kim, C.H., Le Bourhis, X., and Delannoy, P. (2009). GD3 synthase overexpression enhances proliferation and migration of MDA-MB-231 breast cancer cells. Biol. Chem. *390*, 601–609.

Chapman, P.B., Morrisey, D., Panageas, K.S., Williams, L., Lewis, J.J., Israel, R.J., Hamilton, W.B., and Livingston, P.O. (2000). Vaccination with a bivalent G(M2) and G(D2) ganglioside conjugate vaccine: a trial comparing doses of G(D2)-keyhole limpet hemocyanin. Clin. Cancer Res. *6*, 4658–4662.

Chapman, P.B., Williams, L., Salibi, N., Hwu, W.J., Krown, S.E., and Livingston, P.O. (2004). A phase II trial comparing five dose levels of BEC2 anti-idiotypic monoclonal antibody vaccine that mimics GD3 ganglioside. Vaccine *22*, 2904–2909.

Cheever, M.A., Allison, J.P., Ferris, A.S., Finn, O.J., Hastings, B.M., Hecht, T.T., Mellman, I., Prindiville, S.A., Viner, J.L., Weiner, L.M., and Matrisian, L.M. (2009). The prioritization of cancer antigens: a national cancer institute pilot project for the acceleration of translational research. Clin. Cancer Res. *15*, 5323–5337.

Cheung, N.K., Kushner, B.H., Yeh, S.D., and Larson, S.M. (1998). 3F8 monoclonal antibody treatment of patients with stage 4 neuroblastoma: a phase II study. Int. J. Oncol. *12*, 1299–1306.

Daniotti, J.L., Lardone, R.D., and Vilcaes, A.A. (2016). Dysregulated expression of glycolipids in tumor cells: from negative modulator of anti-tumor immunity to promising targets for developing therapeutic agents. Front. Oncol. *5*, 300.

Daniotti, J.L., Vilcaes, A.A., Torres Demichelis, V., Ruggiero, F.M., and Rodriguez-Walker, M. (2013). Glycosylation of glycolipids in cancer: basis for development of novel therapeutic approaches. Front. Oncol. *3*, 306.

Danishefsky, S.J., and Allen, J.R. (2000). From the laboratory to the clinic: a retrospective on fully synthetic carbohydrate-based anticancer vaccines frequently used abbreviations are listed in the appendix. Angew. Chem. Int. Ed. *39*, 836–863.

Dieli, F., Vermijlen, D., Fulfaro, F., Caccamo, N., Meraviglia, S., Cicero, G., Roberts, A., Buccheri, S., D'Asaro, M., Gebbia, N., et al. (2007). Targeting human {gamma}delta} T cells with zoledronate and interleukin-2 for immunotherapy of hormone-refractory prostate cancer. Cancer Res. *67*, 7450–7457.

Doronin, I.I., Vishnyakova, P.A., Kholodenko, I.V., Ponomarev, E.D., Ryazantsev, D.Y., Molotkovskaya, I.M., and Kholodenko, R.V. (2014). Ganglioside GD2 in reception and transduction of cell death signal in tumor cells. BMC Cancer *14*, 295.

Dube, D.H., and Bertozzi, C.R. (2005). Glycans in cancer and inflammation–potential for therapeutics and diagnostics. Nat. Rev. Drug Discov. *4*, 477–488.

Efremova, M., Finotello, F., Rieder, D., and Trajanoski, Z. (2017). Neoantigens generated by individual mutations and their role in cancer immunity and immunotherapy. Front. Immunol. *8*, 1679.

Esser, R., Muller, T., Stefes, D., Kloess, S., Seidel, D., Gillies, S.D., Aperlo-Iffland, C., Huston, J.S., Uherek, C., Schonfeld, K., et al. (2012). NK cells engineered to express a GD2 -specific antigen receptor display built-in ADCC-like activity against tumour cells of neuroectodermal origin. J. Cell Mol. Med. *16*, 569–581.

Fest, S., Huebener, N., Weixler, S., Bleeke, M., Zeng, Y., Strandsby, A., Volkmer-Engert, R., Landgraf, C., Gaedicke, G., Riemer, A.B., et al. (2006). Characterization of GD2 peptide mimotope DNA vaccines effective against spontaneous neuroblastoma metastases. Cancer Res. *66*, 10567–10575.

Furukawa, K., Hamamura, K., Aixinjueluo, W., and Furukawa, K. (2006). Biosignals modulated by tumor-associated carbohydrate antigens: novel targets for cancer therapy. Ann. N. Y. Acad. Sci. *1086*, 185–198.

Gagnon, M., and Saragovi, H.U. (2002). Gangliosides: therapeutic agents or therapeutic targets? Expert Opin. Ther. Patents *12*, 1215–1223.

Grayson, G., and Ladisch, S. (1992). Immunosuppression by human gangliosides. II. Carbohydrate structure and inhibition of human NK activity. Cell Immunol. *139*, 18–29.

Gulley, J.L., Madan, R.A., Pachynski, R., Mulders, P., Sheikh, N.A., Trager, J., and Drake, C.G. (2017). Role of antigen spread and distinctive characteristics of immunotherapy in cancer treatment. J. Natl. Cancer Inst. *109*, https://doi.org/10.1093/jnci/djw261.

Hakomori, S. (2001). Tumor-associated carbohydrate antigens defining tumor malignancy: basis for development of anti-cancer vaccines. Adv. Exp. Med. Biol. *491*, 369–402.

Hamamura, K., Tsuji, M., Hotta, H., Ohkawa, Y., Takahashi, M., Shibuya, H., Nakashima, H., Yamauchi, Y., Hashimoto, N., Hattori, H., et al. (2011). Functional activation of Src family kinase yes protein is essential for the enhanced malignant properties of human melanoma cells expressing ganglioside GD3. J. Biol. Chem. *286*, 18526–18537.

Heimburg-Molinaro, J., Lum, M., Vijay, G., Jain, M., Almogren, A., and Rittenhouse-Olson, K. (2011). Cancer vaccines and carbohydrate epitopes. Vaccine *29*, 8802–8826.

Hoft, D.F., Brown, R.M., and Roodman, S.T. (1998). Bacille Calmette-Guerin vaccination enhances human gamma delta T cell responsiveness to mycobacteria suggestive of a memory-like phenotype. J. Immunol. *161*, 1045–1054.

Horwacik, I., Kurcinski, M., Bzowska, M., Kowalczyk, A.K., Czaplicki, D., Kolinski, A., and Rokita, H. (2011). Analysis and optimization of interactions between peptides mimicking the GD2 ganglioside and the monoclonal antibody 14G2a. Int. J. Mol. Med. *28*, 47–57.

Huang, Y., Yang, Z., Huang, C., McGowan, J., Casper, T., Sun, D., Born, W.K., and O'Brien, R.L. (2015). Gammadelta T cell-dependent regulatory T cells prevent the development of autoimmune keratitis. J. Immunol. *195*, 5572–5581.

Ito, A., Handa, K., Withers, D.A., Satoh, M., and Hakomori, S. (2001). Binding specificity of siglec7 to disialogangliosides of renal cell carcinoma: possible role of disialogangliosides in tumor progression. FEBS Lett. *504*, 82–86.

Iwabuchi, K., Zhang, Y., Handa, K., Withers, D.A., Sinay, P., and Hakomori, S. (2000). Reconstitution of membranes simulating "glycosignaling domain" and their susceptibility to lyso-GM3. J. Biol. Chem. *275*, 15174–15181.

Iwasaki, M., Tanaka, Y., Kobayashi, H., Murata-Hirai, K., Miyabe, H., Sugie, T., Toi, M., and Minato, N. (2011). Expression and function of PD-1 in human gammadelta T cells that recognize phosphoantigens. Eur. J. Immunol. *41*, 345–355.

Kawashima, I., Yoshida, Y., Taya, C., Shitara, H., Yonekawa, H., Karasuyama, H., Tada, N., Furukawa, K., and Tai, T. (2003). Expansion of natural killer cells in mice transgenic for IgM antibody to ganglioside GD2: demonstration of prolonged survival after challenge with syngeneic tumor cells. Int. J. Oncol. *23*, 381–388.

Khan, M.W., Eberl, M., and Moser, B. (2014). Potential use of gammadelta T cell-based vaccines in cancer immunotherapy. Front. Immunol. *5*, 512.

Kim, S.K., Wu, X., Ragupathi, G., Gathuru, J., Koide, F., Cheung, N.K., Panageas, K., and Livingston, P.O. (2011). Impact of minimal tumor burden on antibody response to vaccination. Cancer Immunol. Immunother. *60*, 621–627.

Kirkwood, J.M., Ibrahim, J.G., Sosman, J.A., Sondak, V.K., Agarwala, S.S., Ernstoff, M.S., and Rao, U. (2001). High-dose interferon alfa-2b significantly prolongs relapse-free and overall survival compared with the GM2-KLH/QS-21 vaccine in patients with resected stage IIB-III melanoma: results of intergroup trial E1694/S9512/C509801. J. Clin. Oncol. *19*, 2370–2380.

Kozbor, D. (2010). Cancer vaccine with mimotopes of tumor-associated carbohydrate antigens. Immunol. Res. *46*, 23–31.

Liu, Y., McCarthy, J., and Ladisch, S. (2006). Membrane ganglioside enrichment lowers the threshold for vascular endothelial cell angiogenic signaling. Cancer Res. *66*, 10408–10414.

Minasian, L.M., Yao, T.J., Steffens, T.A., Scheinberg, D.A., Williams, L., Riedel, E., Houghton, A.N., and Chapman, P.B. (1995). A phase I study of anti-GD3 ganglioside monoclonal antibody R24 and recombinant human macrophage-colony stimulating factor in patients with metastatic melanoma. Cancer *75*, 2251–2257.

Morita, C.T., Verma, S., Aparicio, P., Martinez, C., Spits, H., and Brenner, M.B. (1991). Functionally distinct subsets of human gamma/delta T cells. Eur. J. Immunol. *21*, 2999–3007.

Nakashima, H., Hamamura, K., Houjou, T., Taguchi, R., Yamamoto, N., Mitsudo, K., Tohnai, I., Ueda, M., Urano, T., Furukawa, K., and Furukawa, K. (2007). Overexpression of caveolin-1 in a human melanoma cell line results in dispersion of ganglioside GD3 from lipid rafts and alteration of leading edges, leading to attenuation of malignant properties. Cancer Sci. *98*, 512–520.

Navid, F., Santana, V.M., and Barfield, R.C. (2010). Anti-GD2 antibody therapy for GD2-expressing tumors. Curr. Cancer Drug Dargets *10*, 200–209.

Ott, P.A., Hu, Z., Keskin, D.B., Shukla, S.A., Sun, J., Bozym, D.J., Zhang, W., Luoma, A., Giobbie-Hurder, A., Peter, L., et al. (2017). An immunogenic personal neoantigen vaccine for patients with melanoma. Nature *547*, 217–221.

Park, J.E., Wu, D.Y., Prendes, M., Lu, S.X., Ragupathi, G., Schrantz, N., and Chapman, P.B. (2008). Fine specificity of natural killer T cells against GD3 ganglioside and identification of GM3 as an inhibitory natural killer T-cell ligand. Immunology *123*, 145–155.

Paul, S., and Lal, G. (2016). Regulatory and effector functions of gamma-delta (gammadelta) T cells and their therapeutic potential in adoptive cellular therapy for cancer. Int. J. Cancer *139*, 976–985.

Poon, V.I., Roth, M., Piperdi, S., Geller, D., Gill, J., Rudzinski, E.R., Hawkins, D.S., and Gorlick, R. (2015). Ganglioside GD2 expression is maintained upon recurrence in patients with osteosarcoma. Clin. Sarcoma Res. *5*, 4.

Ragupathi, G., Cappello, S., Yi, S.S., Canter, D., Spassova, M., Bornmann, W.G., Danishefsky, S.J., and Livingston, P.O. (2002). Comparison of antibody titers after immunization with monovalent or tetravalent KLH conjugate vaccines. Vaccine *20*, 1030–1038.

Ragupathi, G., Livingston, P.O., Hood, C., Gathuru, J., Krown, S.E., Chapman, P.B., Wolchok, J.D., Williams, L.J., Oldfield, R.C., and Hwu, W.J. (2003). Consistent antibody response against ganglioside GD2 induced in patients with melanoma by a GD2 lactone-keyhole limpet hemocyanin conjugate vaccine plus immunological adjuvant QS-21. Clin. Cancer Res. *9*, 5214–5220.

Ragupathi, G., Meyers, M., Adluri, S., Howard, L., Musselli, C., and Livingston, P.O. (2000). Induction of antibodies against GD3 ganglioside in melanoma patients by vaccination with GD3-lactone-KLH conjugate plus immunological adjuvant QS-21. Int. J. Cancer *85*, 659–666.

Rapoport, E., Mikhalyov, I., Zhang, J., Crocker, P., and Bovin, N. (2003). Ganglioside binding pattern of CD33-related siglecs. Bioorg. Med. Chem. Lett. *13*, 675–678.

Rodriguez, E., Schetters, S.T.T., and van Kooyk, Y. (2018). The tumour glycocode as a novel immune checkpoint for immunotherapy. Nat. Rev. Immunol. *18*, 204–211.

Saleh, M.N., Khazaeli, M.B., Wheeler, R.H., Allen, L., Tilden, A.B., Grizzle, W., Reisfeld, R.A., Yu, A.L., Gillies, S.D., and LoBuglio, A.F. (1992). Phase I trial of the chimeric anti-GD2 monoclonal antibody ch14.18 in patients with malignant melanoma. Hum. Antibodies Hybridomas *3*, 19–24.

Sheridan, B.S., Romagnoli, P.A., Pham, Q.M., Fu, H.H., Alonzo, F., 3rd, Schubert, W.D., Freitag, N.E., and Lefrancois, L. (2013). Gammadelta T cells exhibit multifunctional and protective memory in intestinal tissues. Immunity *39*, 184–195.

Shibuya, H., Hamamura, K., Hotta, H., Matsumoto, Y., Nishida, Y., Hattori, H., Furukawa, K., Ueda, M., and Furukawa, K. (2012). Enhancement of malignant properties of human osteosarcoma cells with disialyl gangliosides GD2/GD3. Cancer Sci. *103*, 1656–1664.

Shurin, G.V., Shurin, M.R., Bykovskaia, S., Shogan, J., Lotze, M.T., and Barksdale, E.M., Jr. (2001). Neuroblastoma-derived gangliosides inhibit dendritic cell generation and function. Cancer Res. *61*, 363–369.

Slovin, S.F., Ragupathi, G., Adluri, S., Ungers, G., Terry, K., Kim, S., Spassova, M., Bornmann, W.G., Fazzari, M., Dantis, L., et al. (1999). Carbohydrate vaccines in cancer: immunogenicity of a fully synthetic globo H hexasaccharide conjugate in man. Proc. Natl. Acad. Sci. U S A *96*, 5710–5715.

Sriram, V., Cho, S., Li, P., O'Donnell, P.W., Dunn, C., Hayakawa, K., Blum, J.S., and Brutkiewicz, R.R. (2002). Inhibition of glycolipid shedding rescues recognition of a CD1+ T cell lymphoma by natural killer T (NKT) cells. Proc. Natl. Acad. Sci. U S A *99*, 8197–8202.

Sun, L., Middleton, D.R., Wantuch, P.L., Ozdilek, A., and Avci, F.Y. (2016). Carbohydrates as T-cell antigens with implications in health and disease. Glycobiology *26*, 1029–1040.

Terme, M., Dorvillius, M., Cochonneau, D., Chaumette, T., Xiao, W., Diccianni, M.B., Barbet, J., Yu, A.L., Paris, F., Sorkin, L.S., and Birkle, S. (2014). Chimeric

antibody c.8B6 to O-acetyl-GD2 mediates the same efficient anti-neuroblastoma effects as therapeutic ch14.18 antibody to GD2 without antibody induced allodynia. PLoS One *9*, e87210.

Todeschini, A.R., Dos Santos, J.N., Handa, K., and Hakomori, S.I. (2007). Ganglioside GM2-tetraspanin CD82 complex inhibits met and its cross-talk with integrins, providing a basis for control of cell motility through glycosynapse. J. Biol. Chem. *282*, 8123–8133.

Tong, W., Gagnon, M., Sprules, T., Gilbert, M., Chowdhury, S., Meerovitch, K., Hansford, K., Purisima, E.O., Blankenship, J.W., Cheung, N.K., et al. (2010). Small-molecule ligands of GD2 ganglioside, designed from NMR studies, exhibit induced-fit binding and bioactivity. Chem. Biol. *17*, 183–194.

Tong, W., Maira, M., Gagnon, M., and Saragovi, H.U. (2015). Ligands binding to cell surface ganglioside GD2 cause Src-dependent activation of N-methyl-D-aspartate receptor signaling and changes in cellular morphology. PLoS One *10*, e0134255.

Vadhan-Raj, S., Cordon-Cardo, C., Carswell, E., Mintzer, D., Dantis, L., Duteau, C., Templeton, M.A., Oettgen, H.F., Old, L.J., and Houghton, A.N. (1988). Phase I trial of a mouse monoclonal antibody against GD3 ganglioside in patients with melanoma: induction of inflammatory responses at tumor sites. J. Clin. Oncol. *6*, 1636–1648.

Van Rhijn, I., van Berlo, T., Hilmenyuk, T., Cheng, T.Y., Wolf, B.J., Tatituri, R.V., Uldrich, A.P., Napolitani, G., Cerundolo, V., Altman, J.D., et al. (2016). Human autoreactive T cells recognize CD1b and phospholipids. Proc. Natl. Acad. Sci. U S A *113*, 380–385.

Vantourout, P., and Hayday, A. (2013). Six-of-the-best: unique contributions of gammadelta T cells to immunology. Nat. Rev. Immunol. *13*, 88–100.

Wondimu, A., Zhang, T., Kieber-Emmons, T., Gimotty, P., Sproesser, K., Somasundaram, R., Ferrone, S., Tsao, C.Y., and Herlyn, D. (2008). Peptides mimicking GD2 ganglioside elicit cellular, humoral and tumor-protective immune responses in mice. Cancer Immunol. Immunother. *57*, 1079–1089.

Wu, D.Y., Segal, N.H., Sidobre, S., Kronenberg, M., and Chapman, P.B. (2003). Cross-presentation of disialoganglioside GD3 to natural killer T cells. J. Exp. Med. *198*, 173–181.

Yankelevich, M., Kondadasula, S.V., Thakur, A., Buck, S., Cheung, N.K., and Lum, L.G. (2012). Anti-CD3 x anti-GD2 bispecific antibody redirects T-cell cytolytic activity to neuroblastoma targets. Pediatr. Blood Cancer *59*, 1198–1205.

Yoshida, S., Fukumoto, S., Kawaguchi, H., Sato, S., Ueda, R., and Furukawa, K. (2001). Ganglioside G(D2) in small cell lung cancer cell lines: enhancement of cell proliferation and mediation of apoptosis. Cancer Res. *61*, 4244–4252.

Yoshida, S., Kawaguchi, H., Sato, S., Ueda, R., and Furukawa, K. (2002). An anti-GD2 monoclonal antibody enhances apoptotic effects of anti-cancer drugs against small cell lung cancer cells via JNK (c-Jun terminal kinase) activation. Jpn. J. Cancer Res. *93*, 816–824.

Yu, A.L., Gilman, A.L., Ozkaynak, M.F., London, W.B., Kreissman, S.G., Chen, H.X., Smith, M., Anderson, B., Villablanca, J.G., Matthay, K.K., et al. (2010). Anti-GD2 antibody with GM-CSF, interleukin-2, and isotretinoin for neuroblastoma. N. Engl. J. Med. *363*, 1324–1334.

Ziche, M., Morbidelli, L., Alessandri, G., and Gullino, P.M. (1992). Angiogenesis can be stimulated or repressed in vivo by a change in GM3:GD3 ganglioside ratio. Lab. Invest. *67*, 711–715.

STAR★METHODS

KEY RESOURCES TABLE

REAGENT or RESOURCE	SOURCE	IDENTIFIER
Antibodies		
Anti-GD2 (14G2a) monoclonal antibody	Santa-Cruz	Cat# sc-53831 RRID:AB_1123587
Anti-GD3 (R24) monoclonal antibody	Abcam	Cat# ab11779 RRID:AB_298562
FITC-conjugated CD4 (OKT-4)	eBioscience	Cat# 11-0048-41 RRID:AB_1633391
Anti-TCRβ (H57-598)	eBioscience	Cat# 14-5961-81 RRID:AB_467757
Hamster anti-TCRγδ,GL3	eBioscience	Cat# 14-5711-82 RRID:AB_467569
FITC-conjugated anti-mouse CD8	eBioscience	Cat# 11-0083-81 RRID:AB_657765
PE-Cy7 conjugated anti-mouse CD4	eBioscience	Cat# 552775 RRID:AB_394461
AF700 conjugated anti-CD3	eBioscience	Cat# 56-0032-80 RRID:AB_529508
PerCP-e710 conjugated anti-CD4	eBioscience	Cat# 46-0047-41 RRID:AB_1834402
APC-e780 conjugated anti-CD8	eBioscience	Cat# 46-0047-41 RRID:AB_1834402
eFLuor450 conjugated anti-CD25	eBioscience	Cat# 48-0251-80 RRID:AB_10698312
APC-conjugated anti-FoxP3	eBioscience	Cat# 17-5773-80 RRID:AB_469456
PE conjugated anti-TCRγδ	eBioscience	Cat# 12-5711-81 RRID:AB_465933
FITC-conjugated anti-mouse IgG	Sigma	Cat# F0257 RRID:AB_259378
Horseradish peroxidase (HRP)-conjugated anti-mouse IgG	Sigma	Cat# A9044 RRID: AB_258431
FITC-conjugated secondary antibody	BD Bioscience	Cat# 554011 RRID:AB_395207
Anti-CD16/32	BD Bioscience	Cat# 553141 RRID:AB_394656
Chemicals, Peptides, and Recombinant Proteins		
GD2 ganglioside	Advanced ImmunoChemical Inc.	Cat# 9-IG6-b
GD3 ganglioside	Advanced ImmunoChemical Inc	Cat# 9-IG7-b
Mitomycin	Sigma	Cat# M4287
^{3}H thymidine	Sigma	Cat# T4688
Critical Commercial Assays		
EasySep Negative Selection Mouse T Cell Enrichment kit	Stemcell Tech.	Cat# 19751A
Experimental Models: Cell Lines		
EL4 mouse thymoma cells	ATCC	ATCC Cat# TIB-39, RRID:CVCL_0255
LLC1 (Lewis lung carcinoma)	ATCC	ATCC Cat# CRL-1642, RRID:CVCL_4358
B16-F1 melanoma	ATCC	ATCC Cat# CRL-6323, RRID:CVCL_0158
Jurkat cells	ATCC	ATCC Cat# TIB-152, RRID:CVCL_0367
Experimental Models: Organisms/Strains		
C57/Bl6 mice	Harlan	RRID:MGI:5656552

CONTACT FOR REAGENT AND RESOURCE SHARING

Further information and request for resources and reagents should be directed to and will be fulfilled by the Lead Contact, Dr. H. Uri Saragovi (uri.saragovi@mcgill.ca).

EXPERIMENTAL MODEL AND SUBJECT DETAILS

Mice

The animal protocol used was reviewed and approved by the Lady Davis Institute Animal Care Committee and animal experiments were performed according to the guidelines of the Canadian Council on Animal Care. Healthy wild-type female C57/Bl6 mice (10-12 weeks of age, 19-20 g) were purchased from Harlan (Lachine, Quebec, Canada) and used to test the effect of PAMAM-GD2 and PAMAM-GD3 in tumor progression and lung metastasis. A maximum of five mice per cage were kept in a 12-h dark-light cycle with food and water *ad libitum*. For the establishment of experimental groups, littermates were randomly assigned to experimental groups. All the *in vivo* tumors are syngeneic and grow rapidly with 100% successful "take" in all vehicle control-treated animals.

Cell Lines

Mouse thymoma EL4-GD2$^+$ (wild type EL4 cells) and Jurkat leukemia (male origin) are from ATCC. EL4-GD3$^+$ cells resulted from negative selection of EL4-GD2$^+$ using anti-GD2 mAbs, they are clonal and stable. EL4-GD2$^+$ cells express GD2 but not GD3, EL4-GD3$^+$ cells express GD3 but not GD2, and Jurkat cells do not express GD2 or GD3, but express GM1. LLC1 cells (Lewis lung carcinoma, ATCC) express low and heterogeneous levels of GD2 and GD3. LLC1-2E5 were FACS-sorted for high GD3-expression, followed by limiting dilution sub-cloning. B16-GD3$^+$ cellsare B16 melanoma cells (male origin, ATCC) transfected with GD3 synthase under 0.5 mg/ml G418 selection. All cells were grown in RPMI 1640 medium (Wisent) supplemented with 5% fetal bovine serum, 2 mM glutamine, 10 mM Hepes and penicillin/streptomycin at 37°C in 5% CO_2 humidified atmosphere. All cell lines were mycoplasma free and were regularly tested by using a PCR mycoplasma detection kit (Zentech). Cell lines have been thoroughly tested and authenticated by ATCC using morphology, karyotyping, and PCR based approaches.

METHODS DETAILS

p- Aminophenylether-β-D-lactopyranoside (AP-Lac, from Toronto Research Chemicals) was used to enzymatically synthesize water soluble (>20 mg/ml) AP-GD2 and AP-GD3 intermediate carbohydrates (Blixt et al., 2005; Tong et al., 2010). The synthesis of AP-GD2 included 215 μmol of AP-GD3 (4 mM), 295 μmol of UDP-GalNAc (5.4 mM), and 10.5 units of CgtA (construct CJL-30), 10 mM $MnCl_2$ and 24 mM Hepes pH 7.0 in a final volume of 55 ml. The reaction mixture was incubated at 37°C for 6.5 hr. Insoluble material was removed by centrifugation at 27,000g for 15 min and the enzyme was removed by ultrafiltration using a 10 kDa membrane cut off. The filtrate was loaded on SepPak C18 5g column (waters Corp) and the product was eluted with water while unidentified contaminants remained in the column. The product was further purified by anion exchange chromatography on HiTrapQ (GE Healthcare) using a gradient of 0-0.3 M NH_4HCO_3 and by size exclusion chromatography on a Superdex Peptide 10/300 GL column (GE Healthcare).

The measured molecular weights of AP-GD2 (1,218 g/mol) and AP-GD3 (927 g/mol) correspond to expected values. Structures were verified by 1D and 2D NMR spectroscopy and mass spectrometry (EI-MS). The AP-GD2 and AP-GD3 intermediates were purified to >99% purity by size-exclusion chromatography (Superdex 30 16 mm X 85 cm column, GE Health Care) before their application in the synthesis of vaccines by conjugation to a dendrimer scaffold.

Synthesis of PAMAM-GD2 and PAMAM-GD3 Dendrimers

Thiophosgene (2 μl) was added to a stirred solution of AP-GD2 (2 mg) in 80% ethanol (300 μl). After 3 hr at room temperature, thin layer chromatography (ethyl acetate: methanol: water: acetic acid 4:2:1:0.1 v/v) showed that a single product had formed. Concentration to near dryness gave a solid, which was treated with water and filtered. The filter cake was washed with water, and the combined filtrate and washings were freeze-dried to give isothiocyanatophenyl GD2 as white powder (1.8 mg, 90% yield). In a separate flask, the volatiles from a methanol solution of polyamidoamine (PAMAM G0, Dendritech, Inc) were evaporated under reduced pressure, and the resulting residue was dissolved in dimethylformamide (DMF). Isothiocyanatophenyl GD2 (1.8 mg) in DMF (110 μl) was added drop-wise to a stirred DMF solution (100 μl) of *N*,*N*-diisopropylethylamine (0.5 μl) and PAMAM G0 (2 μl of 85.4 μg/μl). The reaction was stirred at room temperature for 20 h, until no starting material was detected by TLC. The mixture was diluted with water and dialyzed against water (MW cutoff 2 kDa, Spectrum Laboratories Inc.). The resulting solution was freeze-dried to give 1.34 mg (80% yield) of PAMAM-GD2 vaccine product as white powder that was further characterized by 1D and 2D NMR spectroscopy. The PAMAM-GD3 vaccine was synthesized from AP-GD3 precursor and PAMAM using a similar process. Syntheses of PAMAM-GD2 and PAMAM-GD3 vaccines were reproduced each at least three times, yielding identical products as determined by TLC and NMR.

The vaccine products are heterogeneous mixtures of different amounts of GD2 moieties conjugated onto PAMAM, ranging from 0-4 and including a fully conjugated tetramer (e.g. see the aromatic region (6 ppm and above) of the ^{1}H NMR). Thus, we further investigated the components of the vaccines. The HPLC of PAMAM-GD2 showed two major peaks which were isolated (peak 1 and peak 2) and subjected to NMR analysis. Peak 1 is a PAMAM-lactose tetramer, having lost the GalNAc and sialic acid residues

and which does not contain GD2 epitopes. Peak 2 is a mixture PAMAM-GD2 with all its components, and contains GD2 epitopes including a tetramer. Quantification of the amount of antigen (AP-GD2) in a PAMAM-GD2 vaccine was done by using a selective anti-GD2 mAb (clone 14G2a) (Figure S3A). The amount (w/w) of GD2-reactive epitopes were quantified in each of the different components of PAMAM-GD2 vaccine mixtures (Figure S3B). The loss of sialic acid and GalNAc residue in peak 1 results in no detection of GD2 epitopes. All other fractions isolated from PAMAM-GD2 mixtures bind to 14G2a, suggesting that those fractions have GD2 content. Quantification from dose-response curves indicates that 49 ± 12% (w/w) is AP-GD2 content in the PAMAM-GD2 vaccine mixture.

It is likely that the carbohydrate portion in peak 1 is cleaved due to acidification during the chemical reaction using thiophosgene, because glycosidic linkages are susceptible to this environment. This generates the mixture in the vaccine. However, it is rather surprising that GalNAc is more susceptible than lactose. In cases when the synthetic procedure was altered, the resulting products had different biophysical properties and did not elicit humoral responses, and for that reason they were discarded.

Immunization

PAMAM-GD2 and PAMAM-GD3 were each injected twice intraperitoneally (50 μg in PBS) ~5-7 days apart. The first vaccination had 10% (v/v) gerbu (an adjuvant), while the second vaccination had no adjuvant. Serum samples were collected (capillary Microvette, Sardstedt) and antibody binding to vaccine products or to native gangliosides were analyzed by flow cytometry and ELISA. Tumor volumes were measured over time, and tissues (lymph node, spleen, lung, primary tumor) were collected at the indicated times. A flowchart of the timelines for *in vivo* vaccination is in Figure 3A. Safety parameters after hyper-vaccination were quantified (vision, learning and memory, Figure S7), as well as blood profiles, enzymes associated with liver or kidney damage, motility, retinal health, wire grip strength, and behavior associated with pain was monitored (data not shown).

Tumor-Prophylactic Studies

C57BL/6 mice were injected with vehicle control or vaccinated intraperitoneally. Depending on the experiment, vaccinations were done either 2 or 4 times (50 μg each time), spaced 5–7 days apart. Three to five days after the last vaccination, tumor cells (EL4-GD2$^+$, EL4-GD3$^+$, ranging from 2x10^5 to 4 x 10^5 cells depending on the experiment and cell type) were injected subcutaneously (at "day 0"). Tumors in the control groups were measurable starting at day 7-10 after tumor inoculation.

Tumor-Therapeutic Studies

For subcutaneous tumor inoculation, mice were injected in the left flank (EL4-GD2$^+$, EL4-GD3$^+$ cells, LLC1-2E5 cells). After ~3-4 days (depending on the experiment) the subcutaneous primary tumor was visible/palpable. At that point the mice were treated with vehicle or vaccine (2 times with PAMAM-GD2 or PAMAM-GD3, 50 μg in PBS), intraperitoneally, 5 days apart (e.g. at days 3 and 8 post-inoculation). For the intravenous tumor inoculation, B16-GD3$^+$ cells (1.25 x 10^5) were injected in the tail vein, to achieve lung metastasis. At days 3 and 8 after inoculation the mice were injected intraperitoneally with vehicle control or vaccine, with an endpoint at day 14 post-tumor inoculation. There are no primary tumors to monitor in this model.

Adoptive T Cell Transfer for Therapeutic Studies

Mice were vaccinated intraperitoneally twice with 50 μg of PAMAM-GD2 or PAMAM-GD3, or with control vehicle. Seven days after the second immunization, T cells from spleen and lymph nodes were prepared using the EasySep Negative Selection Mouse T Cell Enrichment Kit (Stemcell Technologies). C57BL/6 recipient mice that had been inoculated subcutaneously with tumor cells (at day 0) received adoptive transfer of ~4 x 10^6 T cells injected intraperitoneally at day 3. Tumors were measured at the indicated times post-inoculation. Cryosections of primary tumors were used to phenotype the Tumor Infiltrating Lymphocytes (TILs). The ipsilateral inguinal and axillary lymph nodes were dissected and their weights measured as an indication of metastasis. The presence of GD2$^+$ or GD3$^+$ cells in lymph node (i.e. tumor cells) was verified by immunofluorescence in cryosections of the lymph nodes.

Characterization of Sera

Flow Cytometry

2 x 10^5 cells of EL4-GD2$^+$, EL4-GD3$^+$, and Jurkat cells were incubated for 20 min on ice with 2 μL mouse antisera (1:50 dilution) or with positive control anti-GD2 mAb (13 nM, 14G2a; Santa Cruz Biotechnology) or anti-GD3 mAb (13 nM, R24; Abcam), followed by FITC-conjugated anti-mouse IgG secondary (1.8 nM, Sigma). Cells were studied immediately in a flow cytometer (Becton-Dickinson), and data analyzed using CellQuest software. Pre-bleed sera and normal mouse sera were used as negative controls. Jurkat cells (negative for GD2 and GD3) were used as negative control cells.

ELISA

Native gangliosides GD2 or GD3 (Advanced ImmunoChemical Inc.), AP-GD2 or AP-GD3 precursors, or PAMAM-GD2 or PAMAM-GD3 vaccines or native gangliosides were immobilized onto polystyrene Corning Strip Well 96-well plates (10 ng/well, Fisher Scientific), and tested for binding of test sera, negative control pre-bleed sera, or positive control mAbs. Secondary was horseradish peroxidase (HRP)-conjugated anti-mouse IgG (Sigma) and readout was colorimetric assays. All tests were done 3-4 independent times for each serum, in duplicate or triplicate wells. The concentration of the primary antibody was 0.33 nM and the concentration of the secondary antibody was 0.06 nM.

Proliferation and Phenotypic Assays

^{3}H-thymidine Incorporation Assays

As target cells EL4-GD2^{+} and control Jurkat were treated with 25 μg/mL Mitomycin (Sigma) for 1 h to arrest DNA synthesis. Cells were washed three times with media to remove Mitomycin, and cells were plated at 2 x 10^{5} cells/well in 96-well plates. As effector cells single cell suspension of splenocytes were prepared from mice immunized twice and from vehicle-injected control mice. Cells were separated using EasySep Negative Selection Mouse T Cell Enrichment Kit (Stemcell Technologies) to >95% purity. The primary T cells were plated at a target to effector ratio of 1:10 or 1:40. As negative control, primary T cells alone (no stimulating target cells) were cultured, and as positive control T cells were treated with Concanavalin A. After 5-7 days of culture, 0.1 μCi/well ^{3}H-thymidine (Sigma-Aldrich) was added and the ^{3}H-thymidine incorporated in DNA was counted by liquid scintillation. Data are reported as average cpm ± sd.

Phenotype of Cytotoxic T Cells

Parallel cultures (without ^{3}H-thymidine) were used to phenotype the expanding T cells. After 7-10 days of culture flow cytometry was performed on a BD LSR Fortessa using a FITC-conjugated anti-mouse CD8 antibody (eBioscience) and PE-Cy7 conjugated anti-mouse CD4 antibody (BD Biosciences). The EL4 are CD3^{+} TCR γδ $^{+}$ T cells but are CD4 and CD8 negative, and human Jurkat cells do not cross-react with anti-mouse reagents. The final concentration of the primary antibodies is 1.2 nM.

Trypan Blue Exclusion Assays

T cells (40,000 total) purified from PAMAM-GD2 vaccinated or control mice were plated in 24-well plates with 1,000 target cells (target to effector ratio of 1:40). After 7 days, *in vitro*, target cell viability was assessed by staining with 0.1% Trypan Blue, and cells were counted using a hemocytometer. Bright field images were acquired using an Olympus CKX41 microscope and Infinity Analyze software (Lumenera Corporation).

Phenotyping of Freshly Isolated Primary T Cells

T cells were isolated from lymph nodes of vaccinated or control mice using the EasySep Negative Selection Mouse T Cell Enrichment Kit (Stemcell Technologies) as above. Flow cytometry was performed on a BD LSRFortessa using a LIVE/DEAD Fixable Aqua Dead Cell Stain (Thermo), AF700 conjugated anti-CD3 antibody, PerCP-e710 conjugated anti-CD4 antibody, APC-e780 conjugated anti-CD8 antibody, eFluor450 conjugated anti-CD25 antibody, APC-conjugated anti-FoxP3 antibody, PE-conjugated anti-TCRβ antibody, and FITC conjugated anti-TCRγδ antibody (all from eBioscience).

Immunofluorescence of TILs in Tumor Cryosections

Primary tumors were excised from control or adoptively-transferred tumor-bearing mice and immediately washed twice in cold PBS and fixed overnight in 4% PFA at 4°C. After two PBS washes, tumors were cryoprotected (30% sucrose for 48 hr), embedded in Optimal Cutting Temperature (O.C.T) Tissue-Tek compound (Sakura Finetek), and 10 μM cryostat sections were mounted on SuperFrost Plus slides (Fisher). The tissue section was blocked with rat anti-mouse CD16/32 at 10 μg/ml (BD Pharmingen) and 2% normal mouse serum in TBST, then with TBST containing 1% BSA and 2% FCS for 30 min each. Standard immunostaining was done using a 1:100 dilution of a hamster clone GL3 anti-TCR TCRγδ antibody (eBioscience), followed by detection using a FITC-conjugated secondary antibody (BD Bioscience), or FITC conjugated anti-CD8a antibody, anti-CD4 antibody, and anti-TCRβ antibody (all from eBioscience). Similar results were obtained using a different anti-TCRγδ antibody clone UC7-13D5 (not shown). Images were acquired using a Leica DM LB2 microscope, mounted with a Leica DFC350 Fx digital camera and Leica Application Suite V3 software (Leica Microsystems).

Evaluation of Primary Tumor Growth and Metastases

The primary tumors were measured with a digital caliper, and data were analyzed by the equation V (mm^{3}) = 0.5 × $width^{2}$ x length. After euthanasia, metastasis to lymph nodes (homing organ for EL4 tumors) were quantified by dissecting the ipsilateral inguinal and axillary lymph nodes and measuring their weights as an indication of metastasis. Metastasis to lung (homing organ for LLC1-2E5 and B16-GD3^{+} tumors) were quantified by counting tumor nodules using ImageJ software.

QUANTIFICATION AND STATISTICAL ANALYSIS

Statistical parameters including the exact value of "n", the dispersion and precision measures (mean ± SD) and statistical significance are reported in the Figures and Figure Legends. Differences in tumor growth for vaccinated versus control groups were analyzed by two-tailed student t-tests; with significance $p<0.05$ (*), $p< 0.01$ (**) and $p< 0.001$ (***). Elsewhere, one-way ANOVA with Tukey-Kramer Multiple Comparisons Test compared different groups.